A High-Resolution Study of Hippocampal and Medial Temporal Lobe Correlates of Spatial Context and Prospective Overlapping Route Memory

Thackery I. Brown,[1,2,3] Michael E. Hasselmo,[1,2] and Chantal E. Stern[1,2,3]*

ABSTRACT: When navigating our world we often first plan or retrieve an ideal route to our goal, avoiding alternative paths that lead to other destinations. The medial temporal lobe (MTL) has been implicated in processing contextual information, sequence memory, and uniquely retrieving routes that overlap or "cross paths." However, the identity of subregions of the hippocampus and neighboring cortex that support these functions in humans remains unclear. The present study used high-resolution functional magnetic resonance imaging (hr-fMRI) in humans to test whether the CA3/DG hippocampal subfield and parahippocampal cortex are important for processing spatial context and route retrieval, and whether the CA1 subfield facilitates prospective planning of mazes that must be distinguished from alternative overlapping routes. During hr-fMRI scanning, participants navigated virtual mazes that were well-learned from prior training while also learning new mazes. Some routes learned during scanning shared hallways with those learned during pre-scan training, requiring participants to select between alternative paths. Critically, each maze began with a distinct spatial contextual Cue period. Our analysis targeted activity from the Cue period, during which participants identified the current navigational episode, facilitating retrieval of upcoming route components and distinguishing mazes that overlap. Results demonstrated that multiple MTL regions were predominantly active for the contextual Cue period of the task, with specific regions of CA3/DG, parahippocampal cortex, and perirhinal cortex being consistently recruited across trials for Cue periods of both novel and familiar mazes. During early trials of the task, both CA3/DG and CA1 were more active for overlapping than non-overlapping Cue periods. Trial-by-trial Cue period responses in CA1 tracked subsequent overlapping maze performance across runs. Together, our findings provide novel insight into the contributions of MTL subfields to processing spatial context and route retrieval, and support a prominent role for CA1 in distinguishing overlapping episodes during navigational "look-ahead" periods. © 2014 Wiley Periodicals, Inc.

KEY WORDS: dentate gyrus; CA3; CA1; fMRI; navigation

[1] Department of Psychological and Brain Sciences, Boston University, Boston, Massachusetts; [2] Center for Memory and Brain, Boston University, Boston, Massachusetts; [3] Athinoula A. Martinos Center for Biomedical Imaging, Massachusetts General Hospital, Charlestown, Massachusetts

*Correspondence to: Chantal E. Stern, 617.353.1396, Center for Memory and Brain, 2 Cummington Mall, Boston University, Boston, MA 02215, USA. E-mail: chantal@bu.edu

INTRODUCTION

Computational models and convergent data from research in rodents and humans indicate a critical role for the medial temporal lobe (MTL) in representing sequences and various forms of context. In particular, the hippocampus has been implicated in retrieving sequential information (Fortin et al., 2002; Lehn et al., 2009; Ross et al., 2009), supporting prospective sequential retrieval, or forward trajectory "look-ahead," of navigational route components during planning and deliberation (Johnson and Redish, 2007). Computational models (Hasselmo and Eichenbaum, 2005; Hasselmo, 2009; Hasselmo and Stern, 2014), supported by experimental data from rodents (Wood et al., 2000; Lee et al., 2006; Smith and Mizumori, 2006) and humans (Kumaran and Maguire, 2006; Kuhl et al., 2010; Brown et al., 2010, 2012; Brown and Stern, 2013) suggest that contextual information combines with sequential associations in the hippocampus to allow retrieval of specific episodes despite interference from overlapping representations. A fundamental question in humans is which subregions of the hippocampus and adjoining MTL cortex process contextual cues and support prospective retrieval of navigational routes.

Building on prior modeling work and anatomical and functional data (introduced below), we present a theoretical model (summarized in Fig. 1) in which spatial contextual information is relayed from the MTL cortex to cue sequential associative retrieval in the hippocampus. These same contextual signals also serve to gate sequential output of the hippocampus based on the current context or goal-relevant memory.

Within the hippocampus, the combined functions of dentate gyrus (DG), CA3, and CA1 processing is predicted to support context-dependent route memory. Specifically, DG neurons receive spatial and item

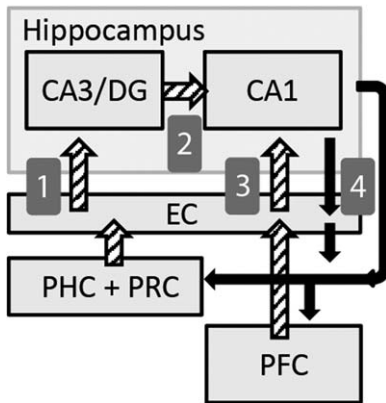**Model of context-dependent memory in the MTL**

FIGURE 1.   Schematic of MTL connectivity and the theoretical relationship between regions in our task. Spatial context and contextual cue scenes are thought to be represented in the parahippocampal cortex (PHC), potentially complemented by landmark object identity signals from perirhinal cortex (PRC). (1) The combined landmark-location cue information is relayed to CA3/DG of the hippocampus via entorhinal cortex (EC). CA3/DG performs associative pattern completion of subsequent learned states in the current environment. The sequential retrieval in CA3/DG converges in CA1 (2) with contextual input relayed from EC (3) which in turn directly receives motivational information from orbitofrontal cortex in the prefrontal cortex (PFC). The convergence of these retrieved states with contextual and goal information in CA1 allows for a gated hippocampal output that reflects the navigational memory that is optimal for the current context. (4) Context-dependent states activated in CA1 are relayed through direct and indirect projections back to PHC and PFC, activating scene memories associated with subsequent states in the environment and influencing behavioral planning.

information and project to region CA3, which is notable for its recurrent excitatory synaptic circuitry (Amaral and Witter, 1989; Van Strien et al., 2009). CA3 is theorized to function as an autoassociative network supporting rapid formation of arbitrary associations, and the subsequent retrieval of sequential associations from the presentation of a cue (McNaughton and Morris, 1987; Treves and Rolls, 1992; Hasselmo and Wyble, 1997; Kesner, 2007). Therefore, the combined CA3/DG subfield is ideally positioned to represent the conjunction of spatial and item information, and replay associated representations when such information is presented as a cue (Mizumori et al., 1999; Carr et al., 2011; Sreenivasan and Fiete, 2011). Consistent with this framework, CA3 neurons in rodents show rapid sequential replay of locations along a route from the current position of the animal (Johnson and Redish, 2007; Davidson et al., 2009).

The CA1 subfield represents a terminal stage of processing in the hippocampal circuit, with output from the CA3/DG circuitry (Fig. 1, path 2) converging with direct input from the entorhinal cortex (van Strien et al., 2009) (Fig. 1, path 3). Models of hippocampal function suggest that the convergence of CA3 and entorhinal information allows CA1 to compute

precise estimates of location (Sreenivasan and Fiete, 2011) and retrieve representations that are most congruent with current context (Hasselmo and Wyble, 1997; Hasselmo and Eichenbaum, 2005). CA1 and CA3/DG subfields may be expected to cooperate in prospective route planning, with spatial contextually-cued associations retrieved by CA3/DG being disambiguated from other navigational memories in CA1. CA1 is thought to be particularly important for prediction of future states in retrieval (Treves, 2004), and neurons in the CA1 subfield show context-dependent firing for locations along overlapping navigational routes based on the prospective path (Wood et al., 2000; Ferbinteanu and Shapiro, 2003; Lee et al., 2006). Importantly, while the subiculum is a key output zone of the hippocampus, CA1 is robustly directly connected to medial and orbitofrontal cortex (Fig. 1, path 4), and feed-forward orbitofrontal projections target medial entorhinal cortex that innervates CA1 (Barbas and Blatt, 1995; Cavada et al., 2000; Rempel-Clower and Barbas, 2000; Barbas, 2007; Roberts et al., 2007; van Strien et al., 2009) (Fig. 1, path 3). These data suggest CA1 activity is positioned to influence and be influenced by goal states, and may be critical for planning and disambiguation of overlapping routes. From this mechanistic perspective, population-level CA3/DG activity would be expected to be elevated for initial contextual retrieval. Activity in CA1, through its role in converting CA3/DG signals into predictive expression of distinct mnemonic episodes, would correlate with overlapping route decision-making.

Contextual memory processing within the subfields of the hippocampus may relate to the neighboring MTL cortex in two critical ways: (1) spatial contextual information (e.g. "where did an event happen?") may be represented by the parahippocampal cortex (Eichenbaum et al., 2007, 2012). In the present experiment, the parahippocampal cortex could be critical for identifying contextually-significant scenes or locations (Epstein and Kanwisher, 1998; O'Craven and Kanwisher, 2000; Burgess et al., 2001; Hartley et al., 2003; Janzen and van Turennout, 2004; Rosenbaum et al., 2004; Epstein and Higgins, 2007; Howard et al., 2011; Mullally and Maguire, 2011; Aminoff et al., 2013) that cue associative retrieval for the current environment in CA3/DG (Fig. 1, path 1) and provides context signals to entorhinal cortex that can gate activity in CA1 (Fig. 1, path 3). (2) Parahippocampal cortex is also the recipient of direct output of CA1 (Blatt and Rosene, 1998), such that mnemonic output of the hippocampus may also support visualization of upcoming states in the environment during planning.

The present high-resolution fMRI study examined human MTL subregions that process spatial contextual cues and support prospective retrieval of navigational route information. In our task, participants navigated a series of virtual routes during fMRI scanning. Some routes shared common hallways with each other, introducing a need to distinguish between, or disambiguate, the mazes during retrieval. Critically, every maze began at a unique spatial location, providing a contextual Cue period during which participants identified the current navigational route and thought forward to the upcoming decision-

points. We examined activations that were specific to the contextual Cue period of the mazes and tested which subregions had Cue period activity relating specifically to prospective retrieval of overlapping route components. We hypothesized that CA3/DG would be particularly important for processing spatial contextual signals and the initial cued forward retrieval of sequential associations identifying the route. Such a role would be reflected in elevated BOLD activity during initial contextual Cue period processing relative to subsequent traversal of individual hallways in the environment. We hypothesized that the parahippocampal cortex would have a similar pattern of Cue-specific activity, supporting the recognition of spatial context underlying prospective hippocampal retrieval, and the visualization of retrieved future locations. We examined whether these correlates differed in magnitude between overlapping and non-overlapping routes during different stages of learning - testing the prediction that contextual retrieval demands during early learning may be greatest for overlapping routes and weakest for non-overlapping routes (Brown and Stern, in press). Finally, we hypothesized that CA1 would be particularly important for the prospective disambiguation of overlapping mazes. Such a role would be reflected in trial-by-trial Cue period BOLD activity, driven by the strength of convergent CA3/DG and contextual/goal state input, correlating with subsequent performance on overlapping decision points.

MATERIALS AND METHODS

Participant Pool

Eighteen participants were recruited for the experiment. Participants were healthy young adults, with no history of neurological or psychiatric disorder. Participants were compensated for their participation at a rate of $10 per hour. Informed consent was obtained from each participant in a manner approved by the Partners Human Research Committee and the Boston University Institutional Review Board. Three participants were excluded due to technical issues with the MRI scanning. A total of 15 participants were included in the final analysis (5 males and 10 females, 2 left handed and 13 right handed). The mean participant age was 21.7 years old (Std. Dev. 3.0 years).

Virtual Navigation Design

Twenty virtual mazes were constructed using POV-Ray Version 3.6.2 (http://www.povray.org/), a three-dimensional raytracer modeling program. Mazes were described to participants as being different routes in an outdoor labyrinth, similar to routes within a city. Participants navigated the virtual routes from a ground-level first-person perspective and behavioral performance (accuracy and reaction time) was recorded using E-Prime 2.0 (Psychology Software Tools, Inc., Pittsburgh, PA). Every maze was comprised of three hallways and three intersec-

tions, such that an equal number of navigational choices and equal linear distances were traveled for each maze. To distinguish locations along the routes, unique, clearly identifiable objects were placed within each intersection.

The twenty mazes were divided into two groups. Ten of the mazes were "overlapping" mazes. Overlapping mazes were split into five pairs that began and ended at distinct, non-overlapping locations, but converged in the middle to share a hallway with another maze (Fig. 2a). The other ten mazes were "non-overlapping", and did not share any hallways or intersections with each other and were therefore completely distinct.

Critical to the experiment, participants began navigation of each maze with a 2 s "Cue period." During the Cue period participants were held stationary in a starting hallway with a view opening into the unique starting intersection of the current maze. During the Cue period, wooden barriers blocked visibility down the subsequent hallways off the intersection so that the only visual information available to participants was the unique landmark of the starting intersection (Fig. 2b). This study targeted MTL activity related to processing spatial contextual cues and planning the upcoming route during the Cue period. Following the Cue period, the wooden barriers fell away and participants could make their initial navigational response for the starting intersection and traverse the subsequent intersections of the maze (Fig. 2c). At each intersection, participants used a button box to turn left, right, or continue straight ahead, selecting the next hall in the sequence of spatial locations comprising a maze. Navigational demands were matched between overlapping and non-overlapping mazes, with the number of left, right, and straight choices counterbalanced across the mazes and experimental conditions.

Following a correct navigational choice, participants would turn down the next hallway and travel to the subsequent intersection. Turns took 1 s. Movement down a hallway was simulated with a video of POV-Ray generated images. Each hallway took 2 s to traverse. Following an incorrect navigational choice, participants received correctional feedback.

The exact timing of the experiment was logged in E-Prime to allow accurate modeling of the task. The total duration of a maze varied with the response times at each intersection. Each maze was followed by an 8 s intertrial interval (ITI) during which participants viewed a fixation point in the center of a black screen.

Experiment Protocol

The experiment was broken into two phases: a prescan training session, followed the next day by the fMRI experiment.

Prescan training

The day before scanning, participants were guided through a sample pair of overlapping routes (different from those used in the actual task) to ensure participants understood the mechanics of the navigational task. Participants were then trained to 100% correct on ten of the virtual routes they would navigate in the scanner ("Old mazes"). Each maze was initially learned
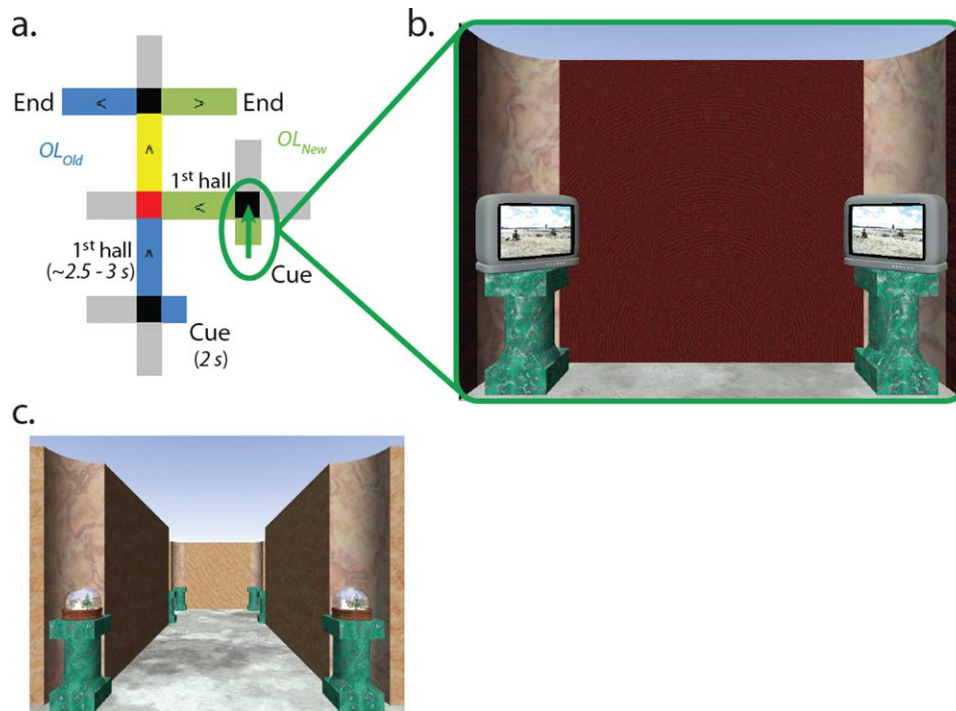
FIGURE 2.   (a) Example of an overlapping route. The OL$_{Old}$ maze is depicted in blue, the OL$_{New}$ maze is depicted in green. The overlapping hallway is highlighted in yellow, and the Critical Decision is highlighted in red. Gray hallways reflect "foil" hallways that appear as viable paths of travel but are never correct choices. The green arrow indicates the Cue period for the OL$_{New}$ maze. (b) Example of the viewpoint during the Cue period. From their starting perspective, participants have a view into the starting intersection. Wooden barriers obstruct the view of the rest of the environment, such that participants can only see the initial starting location landmarks. The initial Cue period identifies which of the overlapping routes is presently being followed, helping participants navigate the intersections entering and exiting the overlapping hallways. (c) Example viewpoint from within an overlapping hallway during active navigation. [Color figure can be viewed in the online issue, which is available at wileyonlinelibrary.com.]

one at a time. Once criterion was met on one maze, participants would learn the next maze. The order in which the ten Old mazes were learned was randomized across participants. Following individual training on the mazes, participants were given five training runs in which all 10 mazes were navigated once per run in a randomized order, similar to the fMRI task they would be given the following day. The final two training runs were required to be error free. Participants were instructed to attend to the Cue period of every maze, as it identified which route they were to follow on a given trial.

The 10 Old mazes were learned as distinct routes which did not overlap with one another. Five of these routes would then become overlapping the following day during fMRI scanning when they came to share common hallways with novel alternative routes (Fig. 2a). The remaining five mazes learned during training would remain non-overlapping during the scanning task. During training, participants did not know which of the Old mazes would become overlapping and which would remain non-overlapping. Participants were instructed during training to simply focus on mastering the ten distinct, currently non-overlapping, routes. Which overlapping and non-overlapping condition mazes were learned during training was randomized across subjects.

Feedback

Participants learned to correctly navigate the virtual mazes by receiving visual feedback for navigational errors: text reading "Wrong!" was overlaid on the scene along with a green arrow indicating the correct direction for that decision point. Participants were then rotated in the correct direction and sent down the correct hall. Participants were allowed a maximum of 5 s to respond at each intersection. "No responses" were treated as incorrect for both the training and scanning components of the study. Participants made few, if any, "no responses" during scanning. Feedback for errors was provided during all components of the study.

fMRI scanning task

Participants performed the fMRI scanning task approximately 24 h and one sleep cycle after prescan training to facilitate consolidation of the mazes learned during training. Before being placed in the scanner, participants were given a warm-up run. During the warm-up run, the 10 Old mazes learned during pre-scan training were navigated once each in a randomized order. Within the scanner, participants performed

10 experimental runs. In each run, participants navigated once through each of the 10 familiar Old mazes, as well as once through each of the 10 novel mazes with which they had no prior experience. Mazes of the different experimental conditions were presented in an interleaved manner. Maze order was counterbalanced across runs, and the order of the runs was randomized across participants. By attending the corrective feedback for errors, participants learned the 10 New mazes across runs.

In non-overlapping mazes, the intersections required the same navigational choices in every trial. In the overlapping mazes, the starting intersections immediately following the Cue period were also always associated with the same navigational choices. However, the second and third intersections were overlapping locations between the mazes. The correct turn at overlapping intersections differed depending on which route was being followed in a given trial (identified by the unique starting Cue location of the maze). We refer to the primary context-dependent decision point (second intersection in the mazes) as the "Critical Decision." Because of its significance as a spatial contextual cue and a key planning period in the task, we focus this report on the Cue period and its relationship to subsequent Critical Decision performance.

The 20 mazes were divided into four experimental conditions for behavioral and fMRI analysis: (1) the five mazes learned during pre-scan training that became overlapping in the scanner comprised the Overlapping$_{Old}$ (OL$_{Old}$) condition. (2) The five mazes learned within the scanner that overlapped with the OL$_{Old}$ routes comprised the Overlapping$_{New}$ (OL$_{New}$) condition. (3) The five mazes learned during pre-scan training that remained non-overlapping in the scanner comprised the Non-overlapping$_{Old}$ (NOL$_{Old}$) condition. (4) The five non-overlapping mazes learned within the scanner comprised the Non-overlapping$_{New}$ (NOL$_{New}$) condition. There were 50 trials per experimental condition.

Postscan interview

After scanning, participants were interviewed about the experimental task. All participants reported using the landmark objects to identify and aid in navigating the virtual routes. As in an earlier whole-brain fMRI study using this experimental paradigm (Brown and Stern, 2013) and related experiments (Brown et al., 2010; Brown et al., 2012), participants reported using the starting Cue period to retrieve the current navigational episode and "think forward" to upcoming context-dependent decisions in the overlapping mazes. We therefore focus this report on the starting Cue period of the mazes and its significance to spatial disambiguation.

Image Acquisition

Images were acquired at the Athinoula A. Martinos Center for Biomedical Imaging of the Massachusetts General Hospital in Charlestown, MA using a 3 Tesla Siemens MAGNETOM TrioTim scanner with a Siemens 32-channel matrix head coil. High resolution T1-weighted multiplanar rapidly acquired gra-

dient echo (MP-RAGE) structural scans were acquired using generalized autocalibrating partially parallel acquisitions (GRAPPA) (TR = 2,530 ms; TE = 3.31 ms; flip angle = 7; slices = 176; resolution = 1 mm isotropic). High-resolution T2*-weighted BOLD images were acquired using an echo planar imaging (EPI) sequence (TR = 2,000 ms; TE = 34 ms; flip angle = 90; slices = 22, resolution = 1.5 × 1.5 × 1.5 mm). Functional image slices were aligned parallel to the long axis of the hippocampus, allowing inclusion of all hippocampal subfields (CA3/DG, CA1, subiculum) and extrahippocampal MTL subregions (perirhinal, entorhinal, and parahippocampal cortices, and the amygdala) in the field of view.

fMRI Preprocessing

Imaging analysis was conducted using SPM8 (Wellcome Department of Cognitive Neurology, London, UK). All BOLD images were reoriented so the origin was 8 mm ventral to the anterior commissure. Images were slice-time corrected to the first slice acquired in time. Motion correction was conducted and included realigning the BOLD images to the first functional image acquired and unwarping the BOLD images to correct for movement-by-susceptibility artifact interactions (Andersson et al., 2001). To further control for the influence of artifacts on our fMRI data, we utilized the Artifact Detection Tools (ART) developed by Shay Mozes and Susan Whitfield-Gabrieli (http://www.nitrc.org/projects/artifact_detect/) to identify signal intensity and combined motion-signal intensity outliers in conjunction with the movement parameters calculated in SPM. Structural images were coregistered with the mean BOLD image obtained during motion correction, segmented into white and gray matter images, and bias-corrected. Because group-level hr-fMRI analysis requires a high-degree of accuracy in intersubject alignment, normalization and cross-participant alignment was conducted following ROI-ANTS procedures developed by the Stark laboratory (described below).

ROI-ANTS—region-of-interest based cross-participant normalization and alignment

We followed procedures established by the Stark laboratory (Yassa et al., 2010, 2011; Lacy et al., 2011) for normalizing and aligning hr-fMRI data across participants with a high degree of accuracy (Yassa and Stark, 2009). The ROI-ANTS procedures involved the following process: an initial whole-brain spatial normalization of each participant's bias-corrected structural images and coregistered BOLD images into Montreal Neurological Institute (MNI) space with SPM provided a rough initial alignment across participants. BOLD images were resampled during normalization to 1 mm^3 isotropic voxels and spatially smoothed with a modest 3 mm full-width at half-maximum Gaussian kernel. We manually delineated each participant's anatomically defined MTL subregions using established protocols (Newmark et al., 2013) based on methods published by the Stark laboratory (Kirwan and Stark, 2007; Kirwan et al., 2007) and guidelines for visualization and

analysis of MTL structures (Insausti et al., 1998; Pruessner et al., 2000, 2002; Zeineh et al., 2000; Duvernoy, 2005; Preston et al., 2010). We defined separate regions of interest (ROIs) for the CA1 subfield, a combined CA3/Dentate Gyrus subregion, subiculum, amygdala, entorhinal cortex, perirhinal cortex, and the parahippocampal cortex. The anatomical ROIs were manually traced on each participant's bias-corrected structural scan using the ITK-SNAP software package (http://www.itksnap.org) (Yushkevich et al., 2006).

The ROI-ANTS methodology uses Advanced Normalization Tools (ANTs), which implements SyN (symmetric normalization), a powerful diffeomorphic registration algorithm (Avants et al., 2008; Klein et al., 2009). A custom template was constructed using ANTS based on the 15 young adult brains in our final participant pool. Each participant's structural scan and subject-specific subregion ROIs were used simultaneously to warp the structural image into the group's custom template space. This approach employed a pure cross-correlation metric to register the grayscale images using cross-correlation optical flow and a point set expectation metric that registered manual subfield label information.

Following estimation of single-subject models (modeling of the data is described below), the ROI-guided structural transformation parameters were applied to the statistical data (parameter estimate maps) to accurately transform the functional data into the template brain space for group-level statistics.

Statistical Analysis of Data

Analysis of behavioral data

Early versus late task phase analysis—scanning day behavior. The present study targeted hr-fMRI data from the Cue period. There was no behavioral performance required for the two second Cue period itself. However, recognition of the starting intersection location and landmarks visible during the Cue period was necessary for the starting intersection navigational choice and the subsequent disambiguation of the routes at the upcoming overlapping choice points. We therefore examined First Intersection and Critical Decision performance for the overlapping and non-overlapping mazes.

Behavioral performance was examined in relation to learning. Specifically, we split the behavioral data into Early and Late trial bins (see Brown and Stern, 2013, and for similar approaches, see Shohamy and Wagner, 2008; Ross et al., 2009). The Early phase was defined as the first three experimental runs, during which learning rates were the greatest for the OL_{New} and NOL_{New} maze Critical Decisions. During this period participants made a comparable number of errors for the two conditions. The Late phase was comprised of the final three runs of the experiment, during which all participants were consistently performing at peak accuracy for the Critical Decision points of each condition.

To examine whether knowledge of the mazes improved comparably from the Early phase to the Late phase in the OL and NOL mazes, average accuracies for the Early and Late bins were entered into a repeated-measures GLM analysis with Task Phase (Early vs. Late) and Condition (OL vs. NOL) as factors. We conducted this analysis separately for the Old and New mazes. An absence of a significant Task Phase by Condition interaction would indicate accuracy changed comparably for the Overlapping and Nonoverlapping conditions from Early to Late trials.

In the OL mazes, interference from the other navigational memory may be expected to prolong the navigational decision-making process, at least for the Critical Decision point of the maze. We therefore also conducted corresponding repeated-measures GLM analyses of the reaction-time data.

hr-fMRI Analyses

Modeling of the navigational task

Individual maze components were modeled based on their conceptually different cognitive processes. Our analysis focused on data from regressors modeling the spatial contextual Cue period, and comparison with navigation of the subsequent First Hallway period. The Cue period was characterized as the initial spatial cue identifying the current navigational episode, and participants report using this period to think beyond the immediate starting intersection choice to the overlapping context-dependent decisions of the upcoming route. These time periods were modeled separately for each condition and training state (OL_{Old}, OL_{New}, NOL_{Old}, and NOL_{New}). To examine how activation differences between the Cue period and subsequent navigation change with learning, for the primary Spatial Contextual Cue-specific Activity and Prospective Disambiguation-related Activity analyses (described below), the Cue and First Hallway periods were separately modeled for Early, Middle, and Late Task Phases of the experiment. As described in the behavioral analysis section above, the Early phase regressors reflected the first three runs, and the Late phase regressors reflected the final three runs.

The Cue period regressors represented the 2 s period in which participants viewed the distinct non-overlapping starting location of each maze without moving. The view of the other hallways was obstructed by wooden barriers during the Cue period. The First Hallway period regressors contained both the time to traverse the first hallway (2 s) and time at the subsequent intersection preceding the primary context-dependent navigational response and the convergence of the routes (∼0.5–1 s). The onsets of the Cue period regressors were separated from the onsets of the First Hallway regressors by an average of 4 s due to the intervening First Intersection choice point and feedback.

In order to accurately capture the variance in the task, additional regressors were created for the remaining maze components for each condition and training state: a First Intersection regressor modeled the time at the starting intersection following the Cue period from the disappearance of the wooden barriers. Secondary Overlapping Decision and Final Hall regressors modeled traversal of the last two hallways of each maze. Because there were no physically overlapping locations

in the non-overlapping mazes, "counterpart" regressors were assigned to the Secondary Overlapping Decision periods for the Non-overlapping condition. An additional regressor modeled the inter-trial intervals (ITI) of the experiment, and a final nuisance regressor accounted for incorrect trials and feedback periods. Finally, the six motion parameters calculated during motion correction, and any time series artifacts identified in ART, were added to the model to account for artifact variance.

Regressors from the task were constructed as a series of square wave functions or "boxcars." Boxcar onsets were defined by the onset of each event, with the duration of Cue period lasting 2 s, and the durations of First Hallway and Secondary Overlapping Decision period boxcars being determined by the reaction time of participants for a particular trial. The Cue period was modeled as a boxcar because we expect processing of the scene and prospective sequence retrieval to occur throughout the 2 s duration. This would predict a proportionally larger hemodynamic response than the response to finite neural activity at the onset of the stimulus (which is reflected by a stick function). These parameters were convolved with the canonical hemodynamic response function in SPM8. The design matrix was then analyzed using the general linear model approach.

Spatial contextual cue-specific activity—Statistical analysis

Our primary group-level statistical analysis targeted activity specific to the contextual cue processing and planning period of overlapping navigational episodes. This analysis was conducted in a manner similar to previous analyses by the Stark group using the ROI-ANTS and ROI-AL methodologies (Kirwan and Stark, 2007; Bakker et al., 2008; Yassa et al., 2011). Specifically, to examine effects that distinguish contextual cue processing and initial prospective retrieval from active navigation and their sensitivity to learning, group analysis began with a two-way Analysis of Variance (ANOVA), with Maze Component (Cue period and the subsequent First Hallway) and Task Phase (Early vs. Late trials) as factors and treating subject as a random effect. Separate ANOVAs were conducted for the New (learned in the scanner) and Old (learned during pre-scan training) overlapping mazes. A voxel-wise threshold of $P < 0.05$ with a spatial extent threshold of 10 voxels was applied to the ANOVA F-statistics. The ANOVAs were conducted within the combined anatomically-defined medial temporal lobe subfield tracings to provide a hybrid functional/anatomical region of interest volume in which to conduct specific follow-up pairwise t-tests of significant main effects and interaction effects (described below).

Follow-up t-tests of significant main effects and interaction effects were conducted in SPM (as opposed to extracting averaged beta weights from each cluster identified in the ANOVA and conducting tests on those values). This approach provided important information about the spatial specificity and location of activations, but retained the across-voxel multiple-comparisons problem common to most fMRI experiments. To control

for the reporting of false positives in the post hoc t-tests, we utilized cluster-extent significance calculations using AlphaSim (from the AFNI software package—http://afni.nimh.nih.gov/afni/), wherein the spatial smoothness of the noise in the data is combined with the number of voxels in the search volume to determine the probability that an activation cluster of size k occurs by chance for a given voxelwise statistical threshold. In our experiment, all pairwise t-tests were conducted with a voxelwise threshold of $P < 0.005$. 10,000 simulation Monte Carlo analyses in AlphaSim identified the cluster extents necessary to maintain family-wise error rates of $P < 0.05$ in our different contrasts.

In the ANOVA, the Maze Component factor compared activity for the overlapping maze Cue periods and the subsequent First Hallways. Both maze components were characterized by the perception of a landmark and location, and memory for the appropriate navigational response for the immediate intersection. However, the Cue period regressor captures activity for the unique starting location of each route, which plays a special role as a spatial contextual cue for the current navigational episode. Participants report that retrieval of the current overlapping route from the unique starting location is characterized by an effort to recollect the upcoming context-dependent decision points. Direct comparison of the Cue period and the subsequent First Hallway identified activations that are specific to processing spatial contextual cues and prospective forward trajectory retrieval beyond the immediate navigational choice during initial route recognition. To this end, significant main effects of Maze Component were examined with specific follow-up paired-sample t-tests contrasting Cue periods with subsequent First Hallways (at $P < 0.005$, cluster significance of $P < 0.05 = k$ of 27). Similarly, significant interactions between Maze Component and Task Phase were explored with specific t-tests contrasting the Early Task Phase Cues with First Hallways, and the Late Task Phase Cues with First Hallways (at $P < 0.005$, cluster significance of $P < 0.05 = k$ of 7).

Because successful navigation of Non-overlapping routes does not require participants to disambiguate the current memory from an alternative route, differences between contextual cue period activity and subsequent navigation may be expected to be particularly strong, at least after continued experience with the route. To examine this possibility, a corresponding analysis of Cue-specific activity was conducted for the non-overlapping mazes.

Prospective disambiguation-related activity—Statistical analysis

Because the ability to distinguish between or disambiguate route memories in our task relied on the unique starting location of each maze, we also conducted an analysis contrasting the level of overlapping maze Cue activity with that for nonoverlapping counterpart mazes. In both conditions participants identify the spatial contextual cue indicating the current route, and the Cue periods are perceptually comparable for the OL

and NOL conditions. But the subject can use associative memory to distinguish the Cue periods of the two conditions. A degree of prospective retrieval is expected to occur in both conditions as a part of having identified which route is currently being navigated, but overlapping maze performance would most directly benefit from explicit look-ahead retrieval of upcoming overlapping choice points as reported by participants.

For this analysis, we used the model from the primary analysis identifying Cue-specific activity. Direct OL > NOL t-test comparisons were made for the Early and Late periods of the task. Because of our strong anatomical prediction that CA1 subfield activity is important for disambiguation during prospective sequence retrieval, an ROI analysis using our manually-delineated CA1 subfield segmentations explicitly tested for activation differences within CA1 (at $P < 0.005$, cluster significance of $P < 0.05 = k$ of 14). We also conducted a conjunction analysis, examining whether any activations specific to the Cue period were also more strongly active for overlapping than non-overlapping maze cues (i.e. OL Cue > NOL Cue contrasts masked to Cue-specific activations) (at $P < 0.005$, cluster significance of $P < 0.05 = k$ of 15). Finally, to determine whether significant correlates of overlapping route planning were specific to the CA1 and Cue-specific ROIs, we also conducted an exploratory analysis of the broader anatomically-defined medial temporal lobe volume at $P < 0.005$, maintaining the cluster-extent threshold of 14.

Prospective cue activity correlated with critical decision performance—Statistical analysis

Modeling work and physiological data led to the prediction that CA1 subfield activity in particular supports prospective disambiguation of overlapping maze components (Hasselmo and Wyble, 1997; Treves, 2004; Hasselmo and Eichenbaum, 2005). To explicitly test this prediction, we conducted a parametric modulation analysis measuring the degree to which trial-by-trial Cue period activity in CA1 correlates with subsequent context-dependent navigational decision performance. Navigational decision accuracy was a binary measure in this task and there were a limited number of error trials, rendering percentage correct a poor measure for this analysis. However, correct Critical Decision trial reaction times provide an effective measure of the degree to which the upcoming navigational response had already been determined by the time participants reach the Critical Decision intersection. The average length of reaction times may be expected to be greater for OL Critical Decisions relative to their counterparts in the NOL mazes due to interference and decision-making demands introduced by alternative navigational memories (examined in behavioral analysis described above), but within each condition trial-by-trial reaction times will vary as a function of the extent to which the decision has been made upon arrival at the intersection.

For the parametric modulation analysis, we created a model with four Cue period regressors (one for each condition: OL_{Old}, OL_{New}, NOL_{Old}, NOL_{New}). Each regressor included all

Cue period trials for that condition, collapsing across runs, which corresponded to correct subsequent Critical Decision trials. In order to measure activations during the Cue period that were greater when subsequent correct Critical Decision reaction times were shorter, parametric modulators for Cue period regressors were created by inverting correct Critical Decision trial reaction times. Reaction times were inverted by dividing the values by the maximum response times for the task (normalizing the data to a range between 0 and 1) and subtracting the resulting number from 1. Reaction times were inverted to facilitate description of significant effects, such that when the hypothesized inverse relationship with reaction time is stronger, this is reflected by more positive values. Importantly, the normalization employed preserves the linear relationships present in the raw data.

The primary parametric modulation analysis was conducted using a targeted region of interest (ROI) approach, testing the prediction that trial-by-trial recruitment of CA1 during the Cue period related to how fast participants respond on subsequent correct context-dependent navigational choices in the mazes (at $P < 0.005$, cluster significance of $P < 0.05 = k$ of 14). To determine whether significant correlates of overlapping route planning were present outside CA1, we also conducted an exploratory analysis of the broader anatomically-defined medial temporal lobe volume at $P < 0.005$, maintaining the same cluster-extent threshold.

Behavioral Results

Early versus late task phase analysis—Scanning day behavior

Behavioral statistics are summarized in Table 1. To help ensure that behavioral accuracy was not a confound when interpreting divergent fMRI activation levels for the Overlapping and Non-overlapping condition from Early to Late trials, average accuracies for the Early and Late bins were entered into a repeated-measures GLM analysis with Task Phase (Early vs. Late) and Condition (OL vs. NOL) as factors. The Task Phase analysis revealed that knowledge of the First Intersection and Critical Decision choice points changed in the same manner from Early trials to Late trials for the Overlapping and Non-overlapping conditions (i.e. the slopes were matched between conditions). Similarly, reaction times changed in the same manner from Early to Late trials for both conditions.

First Intersection accuracy

When comparing OL_{New} and NOL_{New} performance, there was no significant Task Phase by Condition interaction ($F_{(1,14)} = 0.498$, $P = 0.492$), and no main effect of Condition ($F_{(1,14)} = 0.015$, $P = 0.904$). There was a significant main effect of Task Phase ($F_{(1,14)} = 389.911$, $P = 1.3 \times 10^{-11}$). When comparing

TABLE 1.

Behavioral Performance

	New mazes				Old mazes			
	OL		NOL		OL		NOL	
1st Intersections								
Task phase	Accuracy (%)	SEM	Accuracy (%)	SEM	Accuracy (%)	SEM	Accuracy (%)	SEM
Early	62.20	3.30	59.80	3.70	100.00	0.00	99.60	0.04
Late	96.00	2.00	97.80	1.10	99.10	0.09	99.60	0.04
	RT (s)	SEM	RT (s)	SEM	RT (s)	SEM	RT (s)	SEM
Early	1.34	0.11	1.18	0.10	0.64	0.06	0.63	0.05
Late	0.75	0.08	0.64	0.07	0.59	0.07	0.59	0.05
Critical Decisions								
Task phase	Accuracy (%)	SEM	Accuracy (%)	SEM	Accuracy (%)	SEM	Accuracy (%)	SEM
Early	65.80	3.40	66.40	3.00	98.20	1.00	99.10	0.60
Late	96.90	1.30	97.80	1.20	99.10	0.60	99.60	0.40
	RT (s)	SEM	RT (s)	SEM	RT (s)	SEM	RT (s)	SEM
Early	0.94	0.11	0.73	0.08	0.50	0.07	0.46	0.07
Late	0.40	0.03	0.34	0.02	0.42	0.04	0.40	0.03

OL_{Old} and NOL_{Old} performance, there was no significant Task Phase by Condition interaction ($F_{(1,14)} = 0.651$, $P = 0.433$), main effect of Condition ($F_{(1,14)} = 0.000$, $P = 1.000$), or main effect of Task Phase ($F_{(1,14)} = 0.651$, $P = 0.433$).

The First Intersection data ensure that participants had comparable recognition memory across Task Phases for the starting Cue locations of the two conditions.

Critical decision accuracy

When comparing OL_{New} and NOL_{New} performance, there was no significant Task Phase by Condition interaction ($F_{(1,14)} = 0.002$, $P = 0.963$), and no main effect of Condition ($F_{(1,14)} = 0.087$, $P = 0.772$). There was a significant main effect of Task Phase ($F_{(1,14)} = 191.454$, $P = 1.47 \times 10^{-9}$). When comparing OL_{Old} and NOL_{Old} performance, there was no significant Task Phase by Condition interaction ($F_{(1,14)} = 0.318$, $P = 0.582$), main effect of Condition ($F_{(1,14)} = 0.457$, $P = 0.510$), or main effect of Task Phase ($F_{(1,14)} = 3.500$, $P = 0.082$).

First Intersection reaction times

When comparing OL_{New} and NOL_{New} performance, there was no significant Task Phase by Condition interaction ($F_{(1,14)} = 0.310$, $P = 0.586$). There was a significant main effect of Condition ($F_{(1,14)} = 8.439$, $P = 0.012$). There was a significant main effect of Task Phase ($F_{(1,14)} = 37.635$, $p = 2.6 \times 10^{-5}$). These results indicate that reaction times were generally slower for OL_{New} maze first Intersections (despite these being nonoverlapping decision-points in the environment), but improved to the same degree for the Overlapping and Non-overlapping mazes from Early to Late trials. Longer reaction times for OL mazes at this choice point may reflect a bias during the preceding Cue period towards retrieving the upcoming overlapping maze components over the first Intersection choice,

or extended encoding of the current navigational context beyond the Cue period for OL mazes. When comparing OL_{Old} and NOL_{Old} performance, there was no significant Task Phase by Condition interaction ($F_{(1,14)} = 0.061$, $P = 0.808$), main effect of Condition ($F_{(1,14)} = 0.043$, $P = 0.839$), or main effect of Task Phase ($F_{(1,14)} = 1.126$, $P = 0.307$).

Critical decision reaction times

Consistent with increased processing demands relating to disambiguation, reaction times at the Critical Decisions were generally higher for OL_{New} than NOL_{New} mazes. There was no significant Task Phase by Condition interaction ($F_{(1,14)} = 3.075$, $P = 0.103$), but there was a significant main effect of Condition ($F_{(1,14)} = 6.825$, $P = 0.021$). There was a significant main effect of Task Phase ($F_{(1,14)} = 35.749$, $P = 4.6 \times 10^{-5}$). These results indicate that reaction times were generally slower for OL_{New} maze Critical Decisions, but improved to the same degree for the Overlapping and Nonoverlapping mazes from Early to Late trials. When comparing OL_{Old} and NOL_{Old} performance, there was no significant Task Phase by Condition interaction ($F_{(1,14)} = 0.010$, $P = 0.920$), and no main effect of Condition ($F_{(1,14)} = 1.045$, $P = 0.324$). There was a significant main effect of Task Phase ($F_{(1,14)} = 4.764$, $P = 0.047$).

fMRI Results

Spatial cue-specific activity

Multiple regions of the MTL had significant main effects of Maze Component on activity (Cue period and subsequent First Hallway activation differences that did not vary from Early to Late periods of the experiment). Post hoc *t*-tests contrasting Cue period activity with activity during subsequent First Hallway navigation identified several MTL areas that were more strongly active specifically during processing of spatial contextual cues for

TABLE 2.

OL Cue-Specific Activity, Main Effect of Cue > 1st Hall

New mazes			Old mazes		
Subregions	(*t*-value)	(MNI x,y,z)	Subregions	(*t*-value)	(MNI x,y,z)
Activation clusters that overlap between *New* and *Old* mazes					
CA3/DG (left)	4.37	−27, −36, −4	CA3/DG, subiculum, CA1 (left)	3.28	−23, −33, −7
Parahippocampal cortex (left)	6.14	−21, −41, −10	Parahippocampal cortex (left)	6.15	−22, −42, −9
Parahippocampal cortex (right)	5.43	33, −40, −11	Parahippocampal cortex (right)	6.66	35, −35, −16
Perirhinal cortex (left)	3.77	−34, −19, −26	Perirhinal cortex (left)	4.38	−33, −20, −26
Activation clusters that are distinct for *New* and *Old* mazes					
CA1, CA3/DG (right)	3.53	35, −31, −10	Parahippocampal cortex (left)	3.63	−36, −26, −21
Subiculum (right)	4.34	20, −10, −26	Perirhinal cortex (right)	4.90	26, 0, −44
Perirhinal cortex (left)	4.18	−32, −10, −32	-	-	-
Perirhinal cortex (right)	4.58	31, −9, −34	-	-	-

Activations are thesholded at $P < 0.005_{(corr\ P < 0.05)}$. Where multiple regions are listed for a coordinate, the first label corresponds to the region containing the majority of the voxels.

the overlapping routes (Table 2). Of particular interest were MTL areas that had cue-specific activity common to both newly-learned (OL$_{New}$) and well-learned (OL$_{Old}$) mazes: within the hippocampus, a region of the left CA3/DG subfield had activity specific to the spatial contextual Cue period (Fig. 3) for both newly-learned (New) and previously-learned (Old) overlapping mazes. For OL$_{Old}$ mazes the cluster extended into neighboring CA1 and subiculum subfields, with the peak in subiculum. Similarly, bilateral clusters within the parahippocampal cortex and a cluster in the left perirhinal cortex had cue-specific activity common to both newly-learned and well-learned mazes.

Examination of significant interactions between Maze Component and Task Phase identified several subregions of the MTL with Cue-specific activity predominantly during Early or Late periods of the experiment (Table 3). Of note, a region within right perirhinal cortex became more strongly active for the Cue period than for subsequent navigation during the Late task phase for both the newly-learned and previously-learned overlapping routes.

There were no instances of the first hallway leading up to the primary context-dependent decision point having greater activity than the Cue period at $P < 0.005$, corrected, suggesting that initial processing of the navigational context is generally more demanding of the MTL than subsequent active navigation of the first hallway.

As with the analysis of the Overlapping condition, multiple regions of the MTL had significant Cue-specific activity for NOL mazes. Regions with Cue-specific activity common to both newly-learned (NOL$_{New}$) and well-learned (NOL$_{Old}$) mazes across runs were restricted to the MTL cortex (Table 4). As with the OL mazes, bilateral clusters within the parahippocampal cortex and a cluster in the left perirhinal cortex had cue-specific activity common to both newly-learned and well-learned mazes. In contrast to the Overlapping condition, only newly learned NOL mazes had significant Cue-specific hippocampal activity across runs.

Examination of significant interactions between Maze Component and Task Phase (Table 5) indicated that the subiculum was particularly active for the Cue period relative to subsequent navigation during early trials. Furthermore, CA1 became more active for the Cue period with continued practice with Old mazes in the late phase.

Prospective disambiguation-related activity: CA1 ROI analysis

OL > NOL contrasts identified several correlates of cued prospective disambiguation of overlapping routes. The region of interest analysis demonstrated that the CA1 subfield was more strongly active for OL than NOL mazes during the cue period. Activation differences in CA1 for the Early task phase
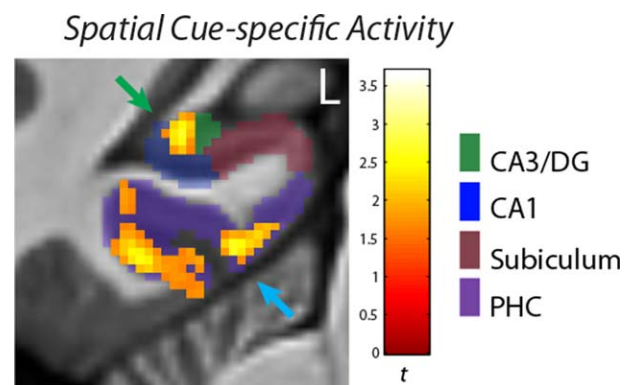

FIGURE 3.   Cue-specific activity. This figure shows OL$_{New}$ activity in the CA3/DG subfield (green arrow) and parahippocampal cortex (blue arrow) that is greater for the initial Cue period than subsequent navigation of the first hallway of the mazes. These clusters also had Cue-specific activity for the OL$_{Old}$ mazes. The activity was thresholded at $P < 0.005_{(corr\ P < 0.05)}$. [Color figure can be viewed in the online issue, which is available at wileyonlinelibrary.com.]

TABLE 3.

OL Cue-Specific Activity, Interaction With Task Phase

New mazes			Old mazes		
Early Cue > 1st hall					
Subregions	**(*t*-value)**	**(MNI x,y,z)**	**Subregions**	**(*t*-value)**	**(MNI x,y,z)**
Activation clusters that are distinct for New and Old mazes					
Entorhinal cortex (left)	4.05	−17, −1, −27	CA1 (left)	5.61	−22, −39, −1
-	-	-	Subiculum (right)	3.87	22, −11, −26
Late Cue > 1st hall					
Subregions	**(*t*-value)**	**(MNI x,y,z)**	**Subregions**	**(*t*-value)**	**(MNI x,y,z)**
Activation clusters that overlap between New and Old mazes					
Perirhinal cortex (right)	3.82	23, 0, −41	Perirhinal cortex (right)	3.90	25, 1, −44
Activation clusters that are distinct for New and Old mazes					
CA3/DG, CA1 (right)	3.95	30, −33, −7	-	-	-
Subiculum (left)	4.89	−20, −33, −9	-	-	-
Parahippocampal cortex (left)	5.33	−20, −41, −10	-	-	-
Parahippocampal cortex (right)	5.56	27, −31, −24	-	-	-
Perirhinal cortex (left)	5.00	−30, −9, −31	-	-	-

Activations are thesholded at $P < 0.005_{(corr\ P < 0.05)}$. Where multiple regions are listed for a coordinate, the first label corresponds to the region containing the majority of the voxels.

were observed in the right hippocampal head ($x, y, z = 17, -8, -23; t = 4.06$) in New mazes (Fig. 4a), and the left hippocampal tail ($x, y, z = -21, -41, -1; t = 5.34$ and $x, y, z = -10, -41, 0; t = 4.60$) for Old mazes (Fig. 4b). Importantly, the left hippocampal tail activation overlapped with the region of CA1 whose trial-by-trial activity correlated with subsequent context-dependent route navigation in Old mazes (see parametric modulation analysis results below). While subthreshold effects should be interpreted with caution, we also note that the same region of CA1 identified for New mazes in the parametric modulation analysis below was also more strongly recruited for OL_{New} than NOL_{New} maze cues during the Late task phase ($x, y, z = 23, -11, -24; t = 5.39$) at a slightly reduced voxel-extent threshold of 10.

TABLE 4.

NOL Cue-Specific Activity, Main Effect of Cue > 1st Hall

New mazes			Old mazes		
Subregions	**(*t*-value)**	**(MNI x,y,z)**	**Subregions**	**(*t*-value)**	**(MNI x,y,z)**
Activation clusters that overlap between New and Old mazes					
Parahippocampal cortex (left)	6.27	−33, −40, −12	Parahippocampal cortex (left)	5.32	−26, −42, −15
Parahippocampal cortex (right)	5.83	34, −39, −11	Parahippocampal cortex (right)	6.64	24, −40, −12
Perirhinal cortex (left)	3.87	−33, −19, −26	Perirhinal cortex (left)	4.46	−34, −11, −30
Activation clusters that are distinct for New and Old mazes					
CA1, CA3/DG (right)	4.03	21, −38, 4	Parahippocampal cortex (left)	4.01	−15, −34, −15
CA1 (right)	4.19	30, −33, −9	-	-	-
CA3/DG (left)	3.45	−21, −38, 0	-	-	-
Subiculum, CA3/DG (left)	3.44	−25, −28, −12	-	-	-

Activations are thesholded at $P < 0.005_{(corr\ P < 0.05)}$. Where multiple regions are listed for a coordinate, the first label corresponds to the region containing the majority of the voxels.

TABLE 5.

NOL Cue-Specific Activity, Interaction With Task Phase

	New mazes			Old mazes	
Early Cue > 1st hall					
Subregions	**(*t*-value)**	**(MNI x,y,z)**	**Subregions**	**(*t*-value)**	**(MNI x,y,z)**
		Activation clusters that are distinct for *New* and *Old* mazes			
Subiculum (left)	3.39	−27, −23, −20	Subiculum (left)	5.18	−17, −34, −5
Subiculum (right)	3.76	15, −37, 0	-	-	-
Late Cue > 1st hall					
Subregions	**(*t*-value)**	**(MNI x,y,z)**	**Subregions**	**(*t*-value)**	**(MNI x,y,z)**
		Activation clusters that are distinct for *New* and *Old* mazes			
-	-	-	CA1 (right)	4.09	20, −13, −20
-	-	-	CA1, Amygdala (left)	3.93	−25, −12, −21
-	-	-	Perirhinal cortex (right)	3.83	21, 3, −37

Activations are thesholded at $P < 0.005_{(corr\ P\ <\ 0.05)}$. Where multiple regions are listed for a coordinate, the first label corresponds to the region containing the majority of the voxels.
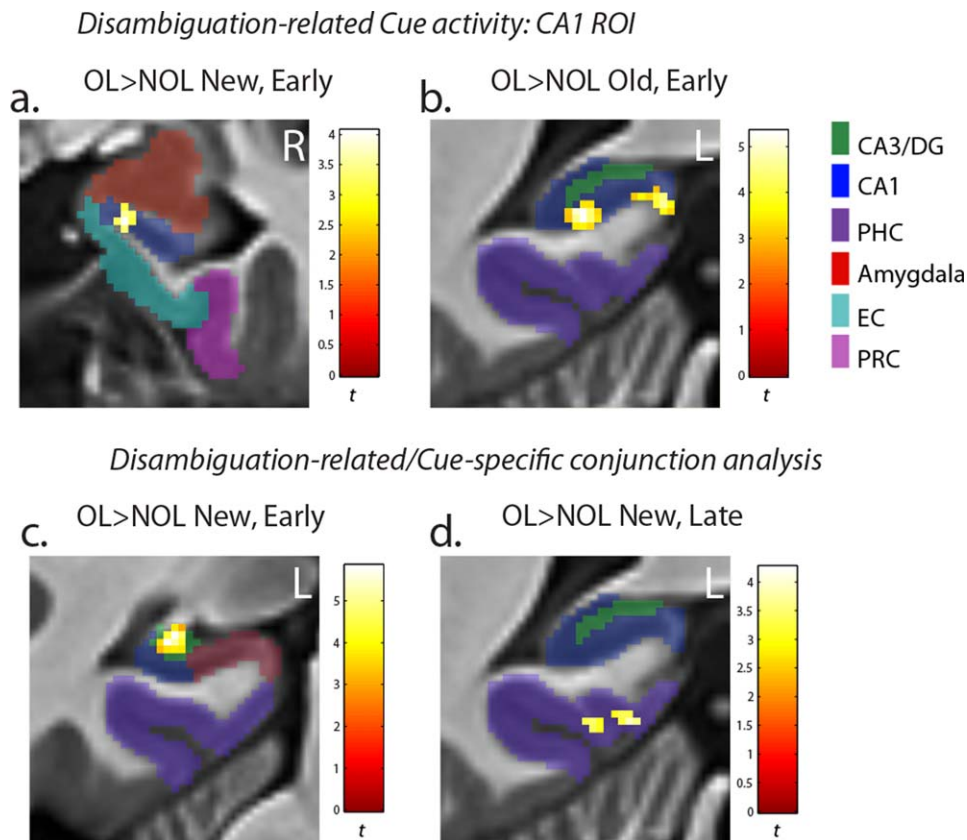

FIGURE 4. Disambiguation-related activity. (a) Within the CA1 region of interest, the rostral CA1 subfield was more strongly active for OL_{New} than NOL_{New} mazes during the initial Cue period of the task in the Early task phase. (b) Within the CA1 region of interest, the posterior CA1 subfield was more strongly active for OL_{Old} than NOL_{Old} mazes during the initial Cue period of the task in the Early task phase. (c) The same region of CA3/DG that had Cue period-specific activity was also more strongly active for OL_{New} than NOL_{New} mazes during the Early task phase. (d) The same region of parahippocampal cortex that was active specifically during the Cue period was also more strongly active for OL_{New} than NOL_{New} mazes during the Late task phase. The activity was thresholded at $P < 0.005_{(corr\ P\ <\ 0.05)}$. [Color figure can be viewed in the online issue, which is available at wileyonlinelibrary.com.]

Disambiguation-Related Activity: Conjunction With Cue-Specific Activity

New mazes			Old mazes		
Early OL Cue > NOL Cue					
Subregions	(*t*-value)	(MNI x,y,z)	Subregions	(*t*-value)	(MNI x,y,z)
Activation clusters that are distinct for New and Old mazes					
CA3/DG	5.83	−27, −34, −6	Parahippocampal cortex	6.60	−33, −35, −17
-	-	-	Parahippocampal cortex	4.68	−33, −37. −11
-	-	-	Parahippocampal cortex	4.24	30, −32, −18
Late OL Cue > NOL Cue					
Subregions	(*t*-value)	(MNI x,y,z)	Subregions	(*t*-value)	(MNI x,y,z)
Activation clusters that are distinct for New and Old mazes					
Parahippocampal cortex	4.25	−30, −27, −22	-	-	-
Parahippocampal cortex	3.88	−17, −40, −12	-	-	-

Activations are thesholded at $p < 0.005$(corr $p < 0.05$).

Prospective disambiguation-related activity: Cue-specific activity conjunction analysis

We also performed a conjunction analysis testing whether regions with activity specific to Cue period of the environment were also more strongly active for overlapping maze cues than non-overlapping maze cues. Significant OL > NOL conjunctive effects were only observed within regions showing positive main effects from the Cue-specific activity analysis (i.e. activations consistently greater for the Cue period than subsequent navigation across task phases) (Table 6). The same region of the left CA3/DG that had Cue-specific activity across all phases of the task was more strongly active for OL_{New} than NOL_{New} cues specifically during the Early task phase (Fig. 4c). This was the only Cue-specific activation to be more strongly active for New OL mazes in the Early task phase, and is consistent with a greater amount of previously learned information about the upcoming OL environment to retrieve from a contextual cue.

In the Late phase of the experiment, disambiguation-related Cue-specific activity for OL_{New} mazes shifted to the parahippocampal cortex (Fig. 4d). For previously-learned OL_{Old} mazes, Cue-specific activity was stronger for OL than NOL mazes specifically within the parahippocampal cortex. These effects were significant during the Early task phase at $P < 0.005$. This disambiguation-related activity localized to a parahippocampal cluster with Cue period-specific activity common to both New and Old mazes.

The exploratory unmasked analysis revealed that the clusters identified in the CA1 ROI and Cue-specific conjunction analyses were the only disambiguation-related activations at $P < 0.005$, maintaining the same cluster extent.

It was interesting that OL > NOL activation differences in the hippocampus generally became non-significant in the Late task phase. Given the increase in Cue-specific activity for familiar NOL_{Old} mazes with continued practice (Table 5), it may be

that cued contextual retrieval becomes greater in Late phases for non-overlapping mazes as the unique representations stabilize, allowing for greater prediction of subsequent states during the initial Cue period. To gain leverage on whether non-significant OL > NOL hippocampal differences in the Late task phase were driven by a decrease in activity for OL mazes, or an increase in activity for NOL mazes, we examined parameter estimates from the regions identified in the disambiguation-specific activity analyses (Fig. 5a–i). Examination of activity from these regions revealed that OL activity in the hippocampal subfields generally only marginally attenuated in the Late task phase, while activity for NOL mazes increased from the Early to Late task phase, supporting the interpretation that initial sequential retrieval of NOL mazes from stable environmental cues may increase with familiarity (Fig. 5a–d). We observed the opposite pattern of activity for the parahippocampal cortex in New mazes (Fig. 5e,f), such that activity for contextual cues remained constant or increased for OL mazes in the Late phase, while activity attenuated for NOL mazes. This could reflect decreasing explicit processing of retrieved future locations for NOL maze route planning.

Prospective Cue Activity Correlated With Critical Decision performance

Trial-by-trial OL_{New} and OL_{Old} Cue-period activity in CA1 was significantly correlated with context-dependent performance at subsequent overlapping intersections (OL_{New}: *x, y, z* = 25, −12, −22, $t = 3.69$; OL_{Old}: *x, y, z* = −26, −40, −1, $t = 4.02$). Notably, the same region of posterior CA1 that was more active for OL_{Old} than NOL_{Old} mazes during Early trials was more strongly active on trials where the subsequent Critical Decision was correctly navigated more quickly. By contrast, there were no significant correlations between Non-overlapping

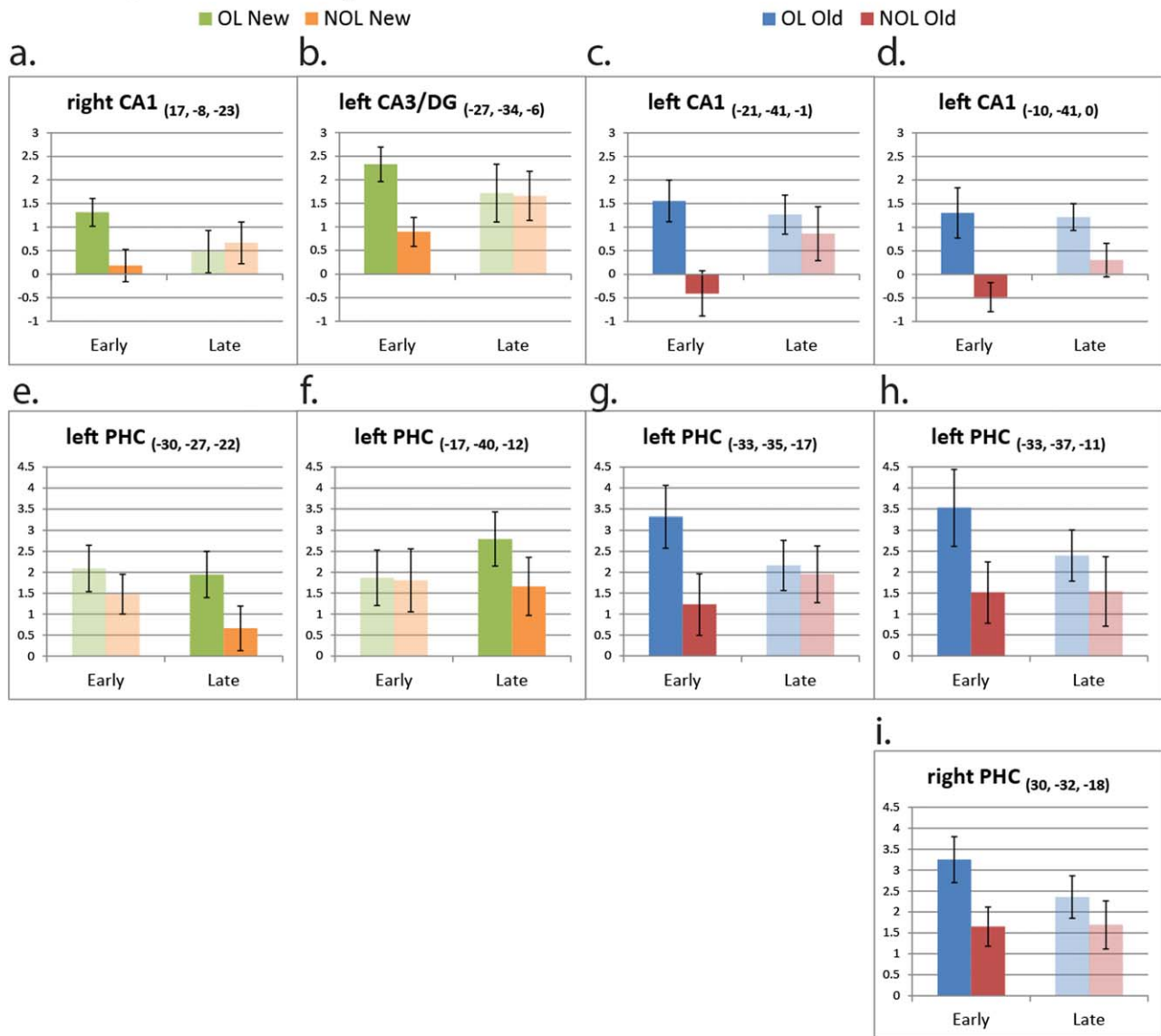## Disambiguation-related parameter estimates

FIGURE 5.   Disambiguation-related parameter estimate extractions (extracted from peak voxels). The graphs illustrate the nature of the relationship between significant OL > NOL activation differences identified in SPM and Task Phase (Early vs. Late). Solid/opaque bars depict parameter estimates from clusters that significantly differ between conditions in SPM ($P < 0.005_{(corr\ P\ <\ 0.05)}$). Translucent bars present parameter estimates from the Task Phase in which the clusters did not significantly differ in SPM. [Color figure can be viewed in the online issue, which is available at wileyonlinelibrary.com.]

maze CA1 activity in the cue period and subsequent navigational performance, consistent with NOL navigation potentially being supported by familiarity or stimulus-response associations.

The exploratory unmasked analysis revealed that CA1 was the only hippocampal subfield with Cue-period activity predictive of subsequent Critical Decision reaction times at $P < 0.005$. In fact, while CA3/DG had prominent Cue-specific and OL > NOL activity identified in the first two analyses, voxels in CA3/DG did not correlate with Critical Decision performance except at a substantially reduced voxelwise statistical threshold of $P < 0.05$ (and at nonsignificant cluster sizes). These findings suggest trial-by-trial processing in CA1 relates most directly to prospective disambiguation and look-ahead success of overlapping routes during the Cue period. Outside CA1, the only MTL regions with activity significantly correlated with subsequent Critical Decision performance at p < 0.005 (with an uncorrected cluster threshold of 14 voxels) were the parahippocampal cortex (OL_{New}: x, y, z = 35, −35, −15, t = 4.50; OL_{Old}: x, y, z = −27, −34, −20, t = 3.63) and posterior medial entorhinal cortex (OL_{New}: x, y, z = −18, −19, −24, t = 4.54).
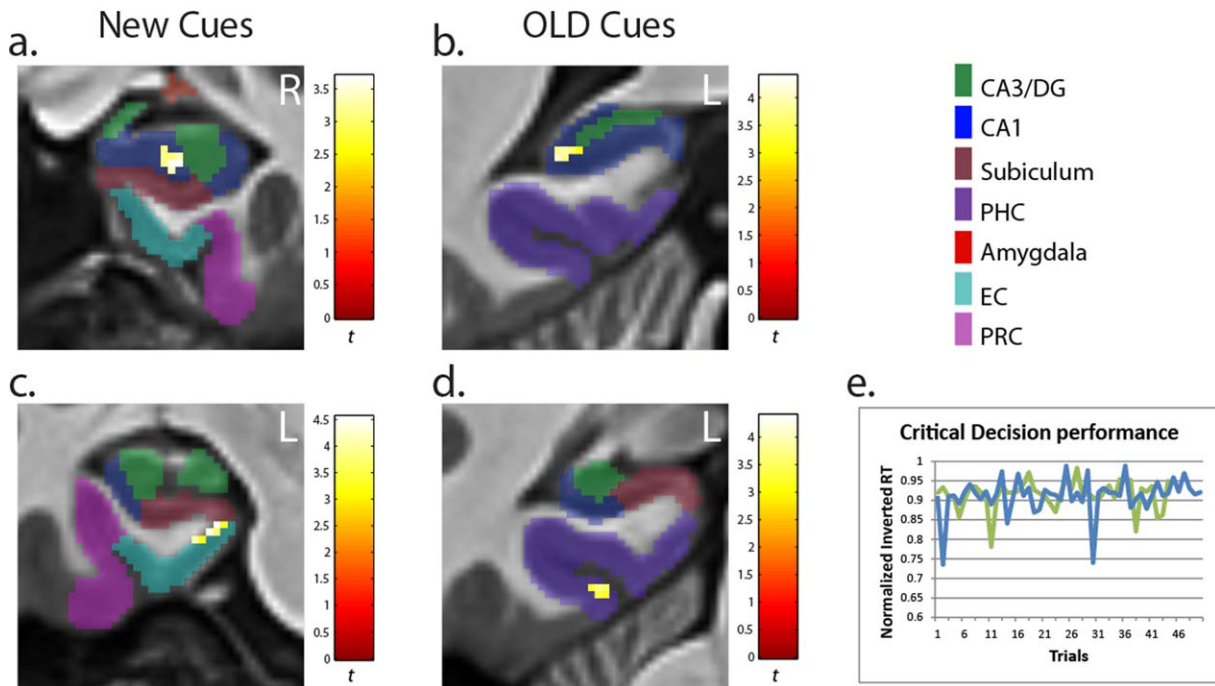
FIGURE 6. Cue period activity parametrically related to subsequent correct Critical Decisions. (a) Across trials, greater activity in the rostral CA1 subfield was correlated with faster subsequent correct Critical Decision reaction times for OL_{New} mazes. (b) Across trials, greater activity in the posterior CA1 subfield was correlated with faster subsequent correct Critical Decision reaction times for OL_{Old} mazes. The parametric modulation analyses were thresholded at $P < 0.005_{(corr \ P < 0.05)}$. (c) Greater activity in the posterior medial entorhinal cortex was also correlated with faster subsequent correct Critical Decision reaction times for OL_{New} mazes ($P < 0.005$, uncorr). (d) Greater activity in the parahippocampal cortex was also correlated with faster subsequent correct Critical Decision reaction times for OL_{Old} mazes ($P < 0.005$, uncorr). (e) Representative example from one subject of OL_{New} (green line) and OL_{Old} (blue line) normalized reaction time parameters underlying this analysis. [Color figure can be viewed in the online issue, which is available at wileyonlinelibrary.com.]

DISCUSSION

The results of this hr-fMRI experiment provide a novel characterization of the MTL system subcomponents involved in spatial contextual cue processing and the initial identification and retrieval of navigational routes in humans. In particular, the CA3/DG subfield of the hippocampus, posterior parahippocampal cortex, and perirhinal cortex had robust activity specific to the spatial contextual cue period across multiple stages of learning and experience in overlapping navigational environments. Activations specific to overlapping maze planning (OL > NOL) localized to the hippocampus predominantly during the Early task phase, driven by limited activity for NOL mazes during this period. Importantly, a region of the left CA3/DG subfield of the hippocampus consistently had activity specific to the Cue period across overlapping maze trials, and Cue period activity in regions of the CA1 subfield tracked prospective disambiguation of subsequent overlapping navigational choices on a trial-by-trial basis.

CA3/DG and Parahippocampal Cortex Process Spatial Contextual Cues

Contextual information plays a central role in episodic memory retrieval and distinguishing between overlapping experiences (Hasselmo and Eichenbaum, 2005; Johnson and Redish, 2007; Zilli and Hasselmo, 2008; Hasselmo, 2009; Brown et al., 2010). Spatial context ("where am I" or "where am I going") may be particularly important to navigational memory (Burgess et al., 2001), but the representation of this information within subregions of the human medial temporal lobes remains poorly understood. Our design allowed us to isolate activity for spatial locations that serve as cues for distinct navigational episodes, and compare this activity with other components of the routes. Critically, voxels in one region of the left CA3/DG subfield had activity specific to the spatial contextual Cue period across Early and Late trials of both the newly-learned and previously-learned Overlapping navigational routes. This finding suggests CA3/DG has a persistent role in processing associations of spatial contextual cues across various stages of experience. Research in rodents has previously implicated CA3/DG circuitry in encoding and processing changes in spatial context (Mizumori et al., 1999;

Hasselmo, 2005; Lee et al., 2005). Importantly, the recurrent CA3/DG circuitry is thought to be important for pattern completion from sparse cue information (McNaughton and Morris, 1987; Treves and Rolls, 1992; Hasselmo et al., 1995; Levy, 1996; Hasselmo and Wyble, 1997; Gold and Kesner, 2005; Kesner, 2007; Tamminga et al., 2010; Chen et al., 2011; Yassa and Stark, 2011), providing a mechanism for encoded environment features and navigational sequences to be retrieved from the unique starting location presented in the Cue period of our task. Importantly, voxels with cue-specific activity were also present in CA1 and the subiculum at various stages of experience with the routes. This is consistent with the interconnectedness of both the neuroanatomy and theoretical functions within hippocampal circuitry (Amaral and Witter, 1989; Van Strien et al., 2009) (Fig. 1). It is striking that within the hippocampus, voxels in one region of left posterior CA3/DG were consistently active for both OL_{New} and OL_{Old} spatial contextual cues throughout our experiment.

The present work is also consistent with an influential theoretical framework in which the parahippocampal cortex provides spatial contextual information to the hippocampal system (Eichenbaum et al., 2007, 2012) (Fig. 1, path 1). Our data build on prior fMRI evidence that parahippocampal cortex activity reflects sequential and spatial associations of scenes (Brown et al., 2010; Turk-Browne et al., 2012). A growing body of literature implicates the parahippocampal cortex in processing scenes, landmarks, and spatial information (Epstein and Kanwisher, 1998; O'Craven and Kanwisher, 2000; Burgess et al., 2001; Hartley et al., 2003; Janzen and van Turennout, 2004; Rosenbaum et al., 2004; Epstein and Higgins, 2007; Howard et al., 2011; Mullally and Maguire, 2011; Brown and Stern, 2013; Sherrill et al., 2013), particularly with their contextual significance (Aminoff et al., 2013). In the present study, both the Cue period and navigation of the 1st hallway of the environment incorporated scene perception, recognition of the upcoming landmarks at a navigational choice-point, and processes relevant to making the immediate navigational choice. Despite these common features, the parahippocampal cortex had robust cue-specific activity across task phases in the Old and New mazes of both OL and NOL conditions. This finding is consistent with the prediction that processing spatial contextual cues, and retrieval of navigationally-relevant associations beyond the immediate scene, is particularly demanding of parahippocampal function.

We also demonstrate cue-specific activity in the perirhinal cortex across task phases for both conditions. The present study was not designed to dissociate parahippocampal and perirhinal cortical functions. However, the similar pattern of activity in these regions can be viewed as consistent with a role for perirhinal cortex in representing item associations and identity (Davachi, 2006; Eichenbaum et al., 2007, 2012; Staresina and Davachi, 2008; Watson et al., 2012). Because place recognition in our task is intimately tied to recognition of the distinct landmark objects at each location, encoding the current navigational context and retrieving

subsequent route elements from the Cue period may in fact rely on the combined function of parahippocampal and perirhinal cortex. In future work, it will be of particular interest to identify the commonalities and differences in functional contributions made by these anatomically-distinct regions of the MTL.

Analysis of the NOL mazes revealed that the CA1 subfield develops Cue-specific activity for familiar (NOL_{Old}) mazes with continued practice. This may indicate that contextual sequence retrieval activity shifts earlier in the mazes as the unique representations stabilize, allowing for greater prediction of subsequent states (while subsequent behavior during active NOL maze navigation may become more habitual). Parameter estimate extractions exploring disambiguation-specific effects (Fig. 5) corroborate a generally increasing pattern of initial Cue period activity from the Early to Late task phase in the hippocampus for the NOL mazes.

Prospective Disambiguation in the Hippocampus and Parahippocampal Cortex

The Cue period of our experiment represents the earliest point in which participants recognize and retrieve the upcoming navigational trial. Therefore, it was of interest to examine Cue activity specifically related to disambiguation of overlapping routes during this period. Standard-resolution fMRI research in humans indicates the hippocampus and parahippocampal cortex are active during initial route planning (Spiers and Maguire, 2006; Viard et al., 2011). In particular, these regions have been shown to be recruited on average for overlapping relative to non-overlapping maze start points (Brown et al., 2010, 2012; Brown and Stern, 2013). In the present experiment, we examined prospective disambiguation activity within the context of learning, examining activation differences in Cue activity separately for Early and Late phases of the experiment. Our conjunction analysis results demonstrate that the same region of the CA3/DG with activity specific to the contextual cue processing period was more strongly active for new overlapping than non-overlapping cues specifically during Early learning trials. Interestingly, after the new mazes had been learned, recruitment of CA3/DG increased for non-overlapping mazes to the same level as the overlapping mazes, suggesting that retrieval processes for non-overlapping route components may occur earlier in navigational trials with increasing familiarity.

CA3/DG circuitry (McNaughton and Morris, 1987; O'Reilly and McClelland, 1994; Hasselmo and Wyble, 1997; Gilbert et al., 2001; Leutgeb et al., 2007; Bakker et al., 2008; Lacy et al., 2011; Yassa and Stark, 2011), and the broader hippocampal complex (Kirwan et al., 2007; Bonnici et al., 2012; LaRocque et al., 2013), has been implicated in pattern separation, whereby representations sharing overlapping features are orthogonalized in memory. Furthermore, CA3/DG has recently been implicated in encoding faces that share overlapping features during working memory (Newmark et al., 2013). Pattern separation may support the disambiguation of navigational

routes. However, the fact that there was persistent recruitment of CA3/DG for the Cue period throughout retrieval phases of our task, the fact that this activity was greater for Cues than during subsequent convergence/overlap of the mazes (First Hallway period), and the fact that recruitment of this region increased for non-overlapping mazes after learning, suggests a different mechanism underlies OL>NOL activation differences in this particular region of CA3/DG. The recurrent circuitry of the CA3/DG has been shown to support one-trial binding of arbitrary associations (McNaughton and Morris, 1987; Treves and Rolls, 1992; Hasselmo and Wyble, 1997; Day et al., 2003; Rolls et al., 2005; Kesner et al., 2008) that can then be retrieved from cues. In our task, CA3/DG could help rapidly bind novel cue locations (OL_{New}) with previously learned information about the environment (OL_{Old}) in support of efficient disambiguation of overlapping routes during early trials of the task. Association between the cues and subsequent decision points was not necessary for non-overlapping maze performance, and there was no existing representation of the NOL_{New} environments prior to entering the scanner, which could limit retrieval-related activity for non-overlapping maze cues during Early trials.

Interestingly, we observed the opposite pattern of activity in the parahippocampal cortex, with activation differences for $OL_{New} > NOL_{New}$ mazes present in Late but not Early trials. Similar parahippocampal activity during early learning of both OL and NOL maze cues is consistent with its more general role in scene encoding (Stern et al., 1996; Epstein et al., 2007; Howard et al., 2011; Mullally and Maguire, 2011), while the divergence in activity after learning to be greater for overlapping maze cues is consistent with evidence that the parahippocampal cortex represents the navigational relevance (Janzen and van Turennout, 2004) and associations of scenes and navigational cues (Brown et al., 2010; Turk-Browne et al., 2012; Brown and Stern, 2013). It will be of interest to design experiments further targeting how navigational features represented in the parahippocampal cortex evolve with continued experience. The fact that the same region of the parahippocampal cortex with activity specific to the Cue period of overlapping mazes was also more active for newly-learned overlapping than non-overlapping maze cues at retrieval suggests that, at least in mazes that are learned as overlapping routes during encoding, the parahippocampal cortex has an important role in the initial retrieval and disambiguation of navigational events.

CA1 Supports Look-ahead to Context-Dependent Navigational Decisions

Consistent with our theoretical framework, our data indicate similar patterns of activity across conditions and task phases for clusters in CA3/DG and CA1. In particular, our OL > NOL CA1 region-of-interest analysis revealed that activity in the CA1 subfield was also more strongly active for overlapping than non-overlapping mazes cues. Importantly, however, our parametric modulation analysis demonstrated that CA1 was the hippocampal subfield with Cue period activity significantly predictive of subsequent Critical Decision performance on a trial-by-trial basis. CA1 has been suggested to play a key role in sequence retrieval and prediction of future states (Treves, 2004), particularly in the prospective disambiguation of overlapping navigational episodes (Hasselmo and Eichenbaum, 2005), and has been associated with pattern completion-like signals and associative retrieval success in humans (Bakker et al., 2008; Chen et al., 2011; Lacy et al., 2011). CA1 has also been associated with learning allocentric representations of space, facilitating navigation to goals from different starting points (Suthana et al., 2012), with flexible access to spatial representations perhaps relating to context-dependent and episodic memory processes. Our parametric modulation analysis demonstrates that the more participants recruited CA1 in a given Cue period trial, the more they had already retrieved the navigational decision, or at least disambiguated the navigational episode, by the time they reached the initial context-dependent choice point in the environment. This correlation is striking because the Cue period was perceptually isolated and separated from the Critical Decision by an intervening navigational choice.

Although the present study was not designed to dissociate contributions of anterior and posterior hippocampal regions, it is also interesting to note that our findings in anterior CA1 for OL_{New} mazes and posterior CA1 for OL_{Old} mazes can be viewed as consistent with a recent theoretical framework (Evensmoen et al., 2013; Poppenk et al., 2013), where coarser or "gist-level" spatial associative retrieval might be predicted in anterior hippocampus for novel and less stable context-dependent memories, while more stable episodic memories (OL_{Old}) may allow for finer-grained retrieval by posterior CA1.

Importantly, the parametric modulation analysis was restricted to Cue period activity corresponding to correct subsequent Critical Decision trials. This indicates the cued context was successfully encoded in the trials underlying this analysis and, coupled with OL > NOL activation differences in these regions of CA1, suggests the correlation is most strongly related to prospective retrieval of the upcoming route. Individual neurons in the CA1 subfield of rodents have been shown to prospectively and uniquely code overlapping locations based on the current navigational episode (Wood et al., 2000; Ferbinteanu and Shapiro, 2003; Lee et al., 2006; Smith and Mizumori, 2006), and CA1 has been associated with maintaining representations with similar features for subsequent use in humans (Newmark et al., 2013). Although speculative, in the framework of our theoretical model the robust Cue period activity observed in the CA3/DG subfield could support encoding incoming contextual cue signals from the MTL cortex (Hasselmo and Eichenbaum, 2005) (Fig. 1, path 1) and non-specific pattern completion of associated environment features (McNaughton and Morris, 1987; Treves and Rolls, 1992; Hasselmo and Wyble, 1997; Gold and Kesner, 2005; Kesner, 2007). Such processes may be critical to retrieving an overlapping route, but their relationship to performance is expected to be indirect—mediated by downstream computations in CA1. The specificity of our lookahead/planning correlate to the CA1 subfield of the hippocampus is consistent with theories

suggesting that it is only through the convergence of CA3/DG and entorhinal cortex information on CA1 (Fig. 1 paths 2 and 3) that the hippocampal system is able to compute precise estimates of location (Sreenivasan and Fiete, 2011) and retrieve representations that are most congruent with current context (Hasselmo and Eichenbaum, 2005). Consequently, the overall pattern of activity in CA3/DG and CA1 is similar between conditions in our task, but additional variance in CA1 relates most directly to future behavior. The relationship between CA1 activity and prospective context-dependent decision-making processes is also consistent with the direct anatomical projections from the CA1 subfield to the prefrontal cortex (Barbas and Blatt, 1995; Cavada et al., 2000; Roberts et al., 2007) and CA1 projections to scene visualization areas like parahippocampal cortex (Blatt and Rosene, 1998).

Within the anatomically and functionally motivated framework put forth in this study (Fig. 1), we expect that if responses in CA1 pyramidal cells are gated by context then BOLD signal measured in CA1 will vary as a function of the number cells active for associative retrieval in CA3/DG, and the strength of contextual input. Additionally, it is possible that through connectivity between CA1 and CA3 (van Strien et al., 2009), and feedback from prefrontal cortex to the hippocampus via entorhinal cortex, repeated activation of cell groups associated with the current episode could further facilitate preferential expression of the appropriate goal-relevant memory.

Beyond the hippocampal system, our exploratory analysis revealed a robust correlation in the parahippocampal cortex with Critical Decision planning for Old mazes, overlapping anatomically with the region more strongly active for overlapping than non-overlapping maze cues. In New mazes, the posterior medial component of the entorhinal cortex had a similar relationship with subsequent performance. This localization of entorhinal activity may be significant because the posterior entorhinal cortex of primates has similar connectivity to the medial entorhinal cortex of rodents (Suzuki and Amarai, 1994; van Strien et al., 2009). The medial entorhinal cortex of rodents contains grid cells which are theorized to be particularly important for spatial memory and may be important for disambiguation processes (Hafting et al., 2005; Lipton et al., 2007; Moser and Moser, 2008; Moser et al., 2008; Hasselmo, 2009; Gupta et al., 2013, in press). In humans, the entorhinal cortex has been implicated in learning (Schon et al., 2004; Suthana et al., 2012). The left entorhinal cortex also had Cue-specific activity during early learning in our task which, combined with the exploratory parametric modulation results, suggests the entorhinal cortex may play a particularly important role in learning and retrieval of novel context-dependent memories.

CONCLUSIONS

Our experiment provides novel insight into the medial temporal lobe mechanisms in humans that process spatial contextual information and facilitate the application of such information to planning and distinguishing between navigational episodes. We show that the CA3/DG subfield of the hippocampus and adjacent parahippocampal and perirhinal cortices are most robustly active for the initial spatially-cued forward trajectory "look-ahead" period relative to subsequent overlapping route navigation. Responses in CA3/DG, CA1, and the parahippocampal cortex are also sensitive to disambiguation demands of the task, being more strongly active for overlapping than nonoverlapping maze contextual cues at different learning stages of the experiment. Consistent with computational models and neuronal recordings in rodents, activity in the CA1 subfield correlated robustly with our measure of prospective disambiguation and route planning. Together, these findings increase our understanding of the role of CA3/DG and CA1 subfields in prospective overlapping route retrieval, and illustrate complementary functions in adjacent medial temporal lobe cortices.

REFERENCES

Amaral DG, Witter MP. 1989. The three-dimensional organization of the hippocampal formation: A review of anatomical data. Neuroscience 31:571–591.

Aminoff EM, Kveraga K, Bar M. 2013. The role of the parahippocampal cortex in cognition. Trends Cogn Sci 17:379–390.

Andersson JL, Hutton C, Ashburner J, Turner R, Friston K. 2001. Modeling geometric deformations in EPI time series,. Neuroimage: 903–919.

Avants BB, Epstein CL, Grossman M, Gee JC. 2008. Symmetric diffeomorphic image registration with cross-correlation: Evaluating automated labeling of elderly and neurodegenerative brain. Med Image Anal 12:26–41.

Bakker A, Kirwan CB, Miller M, Stark CE. 2008. Pattern seperation in the human hippocampal CA3 and dentate gyrus. Science 80: 1640–1642.

Barbas H. 2007. Specialized elements of orbitofrontal cortex in primates. Ann NY Acad Sci 1121:10–32.

Barbas H, Blatt GJ. 1995. Topographically specific hippocampal projections target functionally distinct prefrontal areas in the rhesus monkey. Hippocampus 5:511–533.

Blatt GJ, Rosene DL. 1998. Organization of direct hippocampal efferent projections to the cerebral cortex of the rhesus monkey: projections from CA1, prosubiculum, and subiculum to the temporal lobe. J Comp Neurol 392:92–114.

Bonnici HM, Kumaran D, Chadwick MJ, Weiskopf N, Hassabis D, Maguire EA. 2012. Decoding representations of scenes in the medial temporal lobes. Hippocampus 22:1143–1153.

Brown TI, Ross RS, Keller JB, Hasselmo ME, Stern CE. 2010. Which way was I going? Contextual retrieval supports the disambiguation of well learned overlapping navigational routes. J Neurosci 30: 7414–7422.

Brown TI, Ross RS, Tobyne SM, Stern CE. 2012. Cooperative interactions betweeen hippocampal and striatal systems support flexible navigation. Neuroimage 60:1316–1330.

Brown TI, Stern CE. 2013 Contributions of medial temporal lobe and striatal memory systems to learning and retrieving overlapping spatial memories. Cereb Cortex. Epub ahead of print, DOI: 10.1093/cercor/bht041.

Burgess N, Maguire EA, Spiers HJ, O'keefe J. 2001. A temporospatial and prefrontal network for retrieving the spatial context of lifelike events. Neuroimage 14:439–453.

Carr MF, Jadhav SP, Frank LM. 2011. Hippocampal replay in the awake state: A potential substrate for memory consolidation and retrieval. Nat Neurosci 14:147–153.

Cavada C, Company T, Tejedor J, Cruz-Rizzolo RJ, Reinoso-Suarez F. 2000. The anatomical connections of the macaque monkey orbitofrontal cortex. A review. Cereb Cortex 10:220–242.

Chen J, Olsen RK, Preston AR, Glover GH, Wagner AD. 2011. Associative retrieval processes in the human medial temporal lobe: Hippocampal retrieval success and CA1 mismatch detection. Learn Mem 18:523–528.

Davachi L. 2006. Item, context and relational episodic encoding in humans. Curr Opin Neurobiol:693–700.

Davidson TJ, Kloosterman F, Wilson MA. 2009. Hippocampal replay of extended experience. Neuron:497–507.

Day M, Langston R, Morris RGM. 2003. Glutamate-receptor-mediated encoding and retrieval of paired-associate learning. Nature 424:205–209.

Duvernoy HM. 2005. The Human Hippocampus: Functional Anatomy, Vascularization and Serial Sections with MRI. Springer.

Eichenbaum H, Sauvage M, Fortin NJ, Komorowski R, Lipton P. 2012. Towards a functional organization of episodic memory in the medial temporal lobe. Neurosci Biobehav Rev 36:1597–1608.

Eichenbaum H, Yonelinas AP, Ranganath C. 2007. The medial temporal lobe and recognition memory. Annu Rev Neurosci 30:123–152.

Epstein R, Higgins JS. 2007. Differential parahippocampal and retrosplenial involvement in three types of visual scene recognition. Cereb Cortex 17:1680–1693.

Epstein R, Kanwisher N. 1998. A cortical representation of the local visual environment. Nat Neurosci 392:598–601.

Epstein RA, Parker WE, Feiler AM. 2007. Where am I now? Distinct roles for parahippocampal and retrosplenial cortices in place recognition. J Neurosci 27:6141–6149.

Evensmoen HR, Lehn H, Xu J, Witter MP, Nadel L, Håberg AK. 2013. The anterior hippocampus supports a coarse, global environmental representation and the posterior hippocampus supports fine-grained, local environmental representations. J Cogn Neurosci 25:1908–1925.

Ferbinteanu J, Shapiro ML. 2003. Prospective and retrospective memory coding in the hippocampus. Neuron 40:1227–1239.

Fortin NJ, Agster KL, Eichenbaum H. 2002. Critical role of the hippocampus in memory for sequences of events. Nat Neurosci:458–462.

Gilbert PE, Kesner RP, Lee I. 2001. Dissociating hippocampal subregions: Double dissociation between dentate gyrus and CA1. Hippocampus 11:626–636.

Gold AE, Kesner RP. 2005. The role of the CA3 subregion of the dorsal hippocampus in spatial pattern completion in the rat. Hippocampus 15:808–814.

Gupta K, Beer NJ, Keller LA, Hasselmo ME. 2013. Medial entorhinal grid cells and head direction cells rotate with a t-maze more often during less recently experienced rotations. Cereb Cortex. Epub ahead of print, DOI: 10.1093/cercor/bht020.

Gupta K, Erdem UM, Hasselmo ME. 2013. Model of grid cell activity demonstrates in vivo entorhinal "look-ahead" properties. Neuroscience 247:395-411.

Hafting T, Fyhn M, Molden S, Moser M-B, Moser EI. 2005. Microstructure of a spatial map in the entorhinal cortex. Nature 436:801–806.

Hartley T, Maguire EA, Spiers HJ, Burgess N. 2003. The well-worn route and the path less traveled: Distinct neural bases of route following and wayfinding in humans. Neuron 37:877–888.

Hasselmo ME. 2005. The role of hippocampal regions CA3 and CA1 in matching entorhinal input with retrieval of associations between objects and context: Theoretical comment on Lee et al. (2005). Behav Neurosci 119:342–345.

Hasselmo ME. 2009. A model of episodic memory: Mental time travel along encoded trajectories using grid cells. Neurobiol Learn Mem 92:559–573.

Hasselmo ME, Eichenbaum H. 2005. Hippocampal mechanisms for the context-dependent retrieval of episodes. Neural Networks 18:1172–1190.

Hasselmo ME, Schnell E, Barkai E. 1995. Dynamics of learning and recall at excitatory recurrent synapses and cholinergic modulation in rat hippocampal region CA3. J Neurosci 15:5249–5262.

Hasselmo ME, Stern CE. 2014. Theta rhythm and the encoding and retrieval of space and time. Neuroimage 85(Pt 2):656–666.

Hasselmo ME, Wyble BP. 1997. Free recall and recognition in a network model of the hippocampus: Simulating effects of scopolamine on human memory function. Behav Brain Res 89:1–34.

Howard LR, Kumaran D, Olafsdottir HF, Spiers HJ. 2011. Double dissociation between hippocampal and parahippocampal responses to object-background context and scene novelty. J Neurosci 31:5253–5261.

Insausti R, Juottonen K, Soininen H, Insausti AM, Partanen K, Vainio P, Laakso MP, Pitkänen A. 1998. MR volumetric analysis of the human entorhinal, perirhinal, and temporopolar cortices. AJNR Am J Neuroradiol 19:659–671.

Janzen G, van Turennout M. 2004. Selective neural representation of objects relevant for navigation. Nat Neurosci 7:673–677.

Johnson A, Redish AD. 2007. Neural ensembles in CA3 transiently encode paths forward of the animal at a decision point. J Neurosci 27:12176–12189.

Kesner RP. 2007. Behavioral functions of the CA3 subregion of the hippocampus. Learn Mem 14:771–781.

Kesner RP, Hunsaker MR, Warthen MW. 2008. The CA3 subregion of the hippocampus is critical for episodic memory processing by means of relational encoding in rats. Behav Neurosci 122:1217–1225.

Kirwan CB, Jones CK, Miller MI, Stark CEL. 2007. High-resolution fMRI investigation of the medial temporal lobe. Hum Brain Mapp 28:959–966.

Kirwan CB, Stark CEL. 2007. Overcoming interference: An fMRI investigation of pattern separation in the medial temporal lobe. Learn Mem 14:625–633.

Klein A, Andersson J, Ardekani BA, Ashburner J, Avants B, Chiang M-C, Christensen GE, Collins DL, Gee J, Hellier P, Song JH, Jenkinson M, Lepage C, Rueckert D, Thompson P, Vercauteren T, Woods RP, Mann JJ, Parsey R V. 2009. Evaluation of 14 nonlinear deformation algorithms applied to human brain MRI registration. Neuroimage 46:786–802.

Kuhl BA, Shah AT, DuBrow S, Wagner AD. 2010. Resistance to forgetting associated with hippocampus-mediated reactivation during new learning. Nat Neurosci 13:501–506.

Kumaran D, Maguire EA. 2006. The dynamics of hippocampal activation during encoding of overlapping sequences. Neuron 49:617–629.

Lacy JW, Yassa MA, Stark SM, Muftuler LT, Stark CEL. 2011. Distinct pattern separation related transfer functions in human CA3/dentate and CA1 revealed using high-resolution fMRI and variable mnemonic similarity. Learn Mem 18:15–18.

LaRocque KF, Smith ME, Carr VA, Witthoft N, Grill-Spector K, Wagner AD. 2013. Global similarity and pattern separation in the human medial temporal lobe predict subsequent memory. J Neurosci 33:5466–5474.

Lee I, Griffin AL, Zilli EA, Eichenbaum H, Hasselmo ME. 2006. Gradual translocation of spatial correlates of neuronal firing in the hippocampus toward prospective reward locations. Neuron 51: 639–650.

Lee I, Hunsaker MR, Kesner RP. 2005. The role of hippocampal subregions in detecting spatial novelty. Behav Neurosci 119:145–153.

Lehn H, Steffenach HA, van Strien NM, Veltman DJ, Witter MP, Håberg AK. 2009. A specific role of the human hippocampus in recall of temporal sequences. J Neurosci:3475–3484.

Leutgeb JK, Leutgeb S, Moser M-B, Moser EI.. 2007. Pattern separation in the dentate gyrus and CA3 of the hippocampus. Science 315:961–966.

Levy WB. 1996. A sequence predicting CA3 is a flexible associator that learns and uses context to solve hippocampal-like tasks. Hippocampus 6:579–590.

Lipton PA, White JA, Eichenbaum H. 2007. Disambiguation of overlapping experiences by neurons in the medial entorhinal cortex. J Neurosci 27:5787–5795.

McNaughton BL, Morris RGM. 1987. Hippocampal synaptic enhancement and information storage within a distributed memory system. Trends Neurosci 10:408–415.

Mizumori SJ, Ragozzino KE, Cooper BG, Leutgeb S. 1999. Hippocampal representational organization and spatial context. Hippocampus 9:444–451.

Moser EI, Kropff E, Moser M-B. 2008. Place cells, grid cells, and the brain's spatial representation system. Annu Rev Neurosci 31:69–89.

Moser EI, Moser M-B. 2008. A metric for space. Hippocampus 18: 1142–1156.

Mullally SL, Maguire EA. 2011. A new role for the parahippocampal cortex in representing space. J Neurosci 31:7441–7449.

Newmark RE, Schon K, Ross RS, Stern CE. 2013. Contributions of the hippocampal subfields and entorhinal cortex to disambiguation during working memory. Hippocampus 23:467-475.

O'Craven KM, Kanwisher N. 2000. Mental imagery of faces and places activates corresponding stimulus-specific brain regions. J Cogn Neurosci:1013–1023.

O'Reilly RC, McClelland JL. 1994. Hippocampal conjunctive encoding, storage, and recall: Avoiding a trade-off. Hippocampus 4:661–682.

Poppenk J, Evensmoen HR, Moscovitch M, Nadel L. 2013. Long-axis specialization of the human hippocampus. Trends Cogn Sci 17: 230–240.

Preston AR, Bornstein AM, Hutchinson JB, Gaare ME, Glover GH, Wagner AD. 2010. High-resolution fMRI of content-sensitive subsequent memory responses in human medial temporal lobe. J Cogn Neurosci 22:156–173.

Pruessner JC, Köhler S, Crane J, Pruessner M, Lord C, Byrne A, Kabani N, Collins DL, Evans AC. 2002. Volumetry of temporopolar, perirhinal, entorhinal and parahippocampal cortex from high-resolution MR images: Considering the variability of the collateral sulcus. Cereb Cortex 12:1342–1353.

Pruessner JC, Li LM, Serles W, Pruessner M, Collins DL, Kabani N, Lupien S, Evans AC. 2000. Volumetry of hippocampus and amygdala with high-resolution MRI and three-dimensional analysis software: Minimizing the discrepancies between laboratories. Cereb Cortex 10:433–442.

Rempel-Clower NL, Barbas H. 2000. The laminar pattern of connections between prefrontal and anterior temporal cortices in the Rhesus monkey is related to cortical structural and function. Cereb Cortex 10:851–865.

Roberts AC, Tomic DL, Parkinson CH, Toeling TA, Cutter DJ, Robbins TW, Everitt BJ. 2007. Forebrain connectivity of the pre-frontal cortex in the marmoset monkey (*Callithrix jacchus*): An anterograde and retrograde tract-tracing study. J Comp Neurol 502:86–112.

Rolls ET, Xiang J, Franco L. 2005. Object, space, and object-space representations in the primate hippocampus. J Neurophysiol 94: 833–844.

Rosenbaum RS, Ziegler M, Winocur G, Grady CL, Moscovitch M. 2004. "I have often walked down this street before". fMRI studies on the hippocampus and other structures during mental navigation of an old environment. Hippocampus:826–835.

Ross RS, Brown TI, Stern CE. 2009. The retrieval of learned sequences engages the hippocampus: Evidence from fMRI. Hippocampus 19:790–799.

Schon K, Hasselmo ME, Lopresti ML, Tricarico MD, Stern CE. 2004. Persistence of parahippocampal representation in the absence of stimulus input enhances long-term encoding: A functional magnetic resonance imaging study of subsequent memory after a delayed match-to-sample task. J Neurosci 24:11088–11097.

Sherrill KR, Erdem UM, Ross RS, Brown TI, Hasselmo ME, Stern CE. 2013. Hippocampus and retrosplenial cortex combine path integration signals for successful navigation. J Neurosci 33:19304–19313.

Shohamy D, Wagner AD. 2008. Integrating memories in the human brain: Hippocampal-midbrain encoding of overlapping events. Neuron 60:378–389.

Smith DM, Mizumori SJ. 2006. Learning-related development of context-specific neuronal responses to places and events: The hippocampal role in context processing. J Neurosci 26:3154–3163.

Spiers HJ, Maguire EA. 2006. Thoughts, behavior, and brain dynamics during navigation in the real world. Neuroimage 31:1826–1840.

Sreenivasan S, Fiete I. 2011. Grid cells generate an analog error-correcting code for singularly precise neural computation. Nat Neurosci 14:1330–1337.

Staresina BP, Davachi L. 2008. Selective and shared contributions of the hippocampus and perirhinal cortex to episodic item and associative encoding. J Cogn Neurosci 20:1478–1489.

Stern CE, Corkin S, González RG, Guimaraes AR, Baker JR, Jennings PJ, Carr CA, Sugiura RM, Vedantham V, Rosen BR. 1996. The hippocampal formation participates in novel picture encoding: Evidence from functional magnetic resonance imaging. Proc Natl Acad Sci USA 93:8660–8665.

Suthana N, Haneef Z, Stern J, Mukamel R, Behnke E, Knowlton B, Fried I. 2012. Memory enhancement and deep-brain stimulation of the entorhinal area. N Engl J Med 366:502–510.

Suzuki WA, Amarai DG. 1994. Topographic organization of the reciprocal connections between the monkey entorhinal cortex and the perirhinal and parahippocampal cortices. J Neurosci 14:1856–1877.

Tamminga CA, Stan AD, Wagner AD. 2010. The hippocampal formation in schizophrenia. Am J Psychiatry 167:1178–1193.

Treves A. 2004. Computational constraints between retrieving the past and predicting the future, and the CA3-CA1 differentiation. Hippocampus 14:539–556.

Treves A, Rolls ET. 1992. Computational constraints suggest the need for two distinct input systems to the hippocampal CA3 network. Hippocampus 2:189–199.

Turk-Browne NB, Simon MG, Sederberg PB. 2012. Scene representations in parahippocampal cortex depend on temporal context. J Neurosci 32:7202–7207.

Van Strien NM, Cappaert NLM, Witter MP. 2009. The anatomy of memory: An interactive overview of the parahippocampal-hippocampal network. Nat Rev Neuroscien 10:272–282.

Viard A, Doeller CF, Hartley T, Bird CM, Burgess N. 2011. Anterior hippocampus and goal-directed spatial decision making. J Neurosci 31:4613–4621.

Watson HC, Wilding EL, Graham KS. 2012. A role for perirhinal cortex in memory for novel object-context associations. J Neurosci 32:4473–4481.

Wood ER, Dudchencko PA, Robitsek RJ, Eichenbaum H. 2000. Hippocampal neurons encode information about different types of memory episodes occurring in the same location. Neuron 27:623–633.

Yassa MA, Mattfeld AT, Stark SM, Stark CEL. 2011. Age-related memory deficits linked to circuit-specific disruptions in the hippocampus. Proc Natl Acad Sci USA 108:8873–8878.

Yassa MA, Stark CEL. 2009. A quantitative evaluation of cross-participant registration techniques for MRI studies of the medial temporal lobe. Neuroimage 44:319–327.

Yassa MA, Stark CEL. 2011. Pattern separation in the hippocampus. Trends Neurosci 34:515–525.

Yassa MA, Stark SM, Bakker A, Albert MS, Gallagher M, Stark CEL. 2010. High-resolution structural and functional MRI of hippocampal CA3 and dentate gyrus in patients with amnestic Mild Cognitive Impairment. Neuroimage 51:1242–1252.

Yushkevich PA, Piven J, Hazlett HC, Smith RG, Ho S, Gee JC, Gerig G. 2006. User-guided 3D active contour segmentation of anatomical structures: Significantly improved efficiency and reliability. Neuroimage 31:1116–1128.

Zeineh MM, Engel SA, Bookheimer SY. 2000. Application of cortical unfolding techniques to functional MRI of the human hippocampal region. Neuroimage 11:668–683.

Zilli EA, Hasselmo ME. 2008. Modeling the role of working memory and episodic memory in behavioral tasks. Hippocampus 18:193–209.